UNIVERSIDADE FEDERAL DE PERNAMBUCO
CENTRO DE TECNOLOGIA E GEOCIÊNICIAS
DEPARTAMENTO DE ENERGIA NUCLEAR
CURSO DE GRADUAÇÃO EM ENGENHARIA DE ENERGIA

João Marcos Oliveira de Senna Caaetê Chacon

EVALUATION OF THE CAMS GRIDDED SOLAR RADIATION MODEL IN BRAZIL

Recife
2025

Documento assinado digitalmente
JOAO MARCOS OLIVEIRA DE SENNA CAAETE CH
Data: 22/04/2025 21:59:19-0300
Verifique em https://validar.iti.gov.br

Autor: _____

João Marcos Oliveira de Senna Caaetê Chacon

EVALUATION OF THE CAMS GRIDDED SOLAR RADIATION MAP IN BRAZIL

Trabalho de Conclusão de Curso apresentado ao Curso de Engenharia de Energia da Universidade Federal de Pernambuco, como requisito parcial para obtenção do título de Engenheiro de Energia.

Documento assinado digitalmente
OLGA DE CASTRO VILELA
Data: 23/04/2025 09:30:53-0300
Verifique em https://validar.iti.gov.br

Orientadora: _____

Profa. Dra. Olga de Castro Vilela

Universidade Federal de Pernambuco

Documento assinado digitalmente
DIEGO RODRIGUES DE MIRANDA
Data: 24/04/2025 14:03:43-0300
Verifique em https://validar.iti.gov.br

Coorientador: _____

MSc. Diego Rodrigues de Miranda

German Aerospace Center

Coorientadora: _____

Digital signiert von Faiza Azam
DN: OU=Institute of Networked Energy Systems, O="German Aerospace Center (DLR)", CN=Faiza Azam, E=faiza.azam@dlr.de
Grund: Letter of support
Ort: Oldenburg
Datum: 2025.04.25 09:52:23+02'00'
Foxit PDF Reader Version: 2024.4.0

Dra. Faiza Azam

German Aerospace Center

Recife

2025

Ficha de identificação da obra elaborada pelo autor,
através do programa de geração automática do SIB/UFPE

Chacon, João Marcos Oliveira de Senna Caaetê.
Evaluation of the cams gridded solar radiation map in Brazil / João Marcos Oliveira de Senna Caaetê Chacon. - Recife, 2025.
54 p. : il., tab.

Orientador(a): Olga de Castro Vilela
Cooorientador(a): Diego Rodrigues de Miranda
Cooorientador(a): Faiza Azam
Trabalho de Conclusão de Curso (Graduação) - Universidade Federal de Pernambuco, Centro de Tecnologia e Geociências, Engenharia de Energia - Bacharelado, 2025.
Inclui referências, apêndices.

1. Radiação solar. 2. CAMS. 3. Mapas em grade. 4. Validação. 5. Brasil. I. Vilela, Olga de Castro. (Orientação). II. Miranda, Diego Rodrigues de. (Coorientação). IV. Azam, Faiza. (Coorientação). V. Título.

620 CDD (22.ed.)

João Marcos Oliveira de Senna Caaetê Chacon

EVALUATION OF THE CAMS GRIDDED SOLAR RADIATION MAP IN BRAZIL

Trabalho de Conclusão de Curso apresentado ao Curso de Engenharia de Energia da Universidade Federal de Pernambuco, como requisito parcial para obtenção do título de Engenheiro de Energia.

Aprovado em: 09/04/2025

BANCA EXAMINADORA

Documento assinado digitalmente
gov.br
ALEXANDRE CARLOS ARAUJO DA COSTA
Data: 25/04/2025 11:03:13-0300
Verifique em https://validar.iti.gov.br

Prof. Dr. Alexandre Carlos Araújo da Costa

Universidade Federal de Pernambuco

Documento assinado digitalmente
gov.br
DORIS REGINA AIRES VELEDA
Data: 25/04/2025 10:35:44-0300
Verifique em https://validar.iti.gov.br

Profa. Dra. Dóris Regina Aires Veleda

Universidade Federal de Pernambuco

I dedicate this work to my God, who took care of me and preserved me during this phase and has given me a purpose to continue.

ACKNOWLEDGEMENTS

During this time there have been many people who have played an active part in my life and I am grateful for the lives of each one of them, for listening to me and supporting me in this phase of life that is coming to an end.

Firstly, I must thank my God, who has been there for me and strengthened me in the most difficult times. He was the one who opened and closed doors, always guiding me and showing me the path I should follow, making me wiser every year to know how to deal with the growing demands that I couldn't even imagine when I started the course.

I am also extremely grateful for the people God has put in my life. My parents, who even though they didn't always know how to help, were always by my side for whatever I needed, even though they were physically distant, I could feel their support so fully. Still in my family, I had my brother, who when I started the course was just a boy, but today I can be proud of how he has matured, and in the process, he has helped me to see things in ways I would never have imagined, but he often showed me how.

Among the things that have changed during this time at university, I can say that one of the main ones was, at the beginning, when I got to know the woman who had been with me all this time. Often listening to my regrets and giving advice, encouraging me to look at what is true and showing me that not everything needs to be so pragmatic. Letícia, my love, thank you for your affection, attention and patience. There couldn't have been a better person to spend time with.

I would like to thank my brothers and sisters who were by my side and prayed for me during this time, the PG members, friends from the youth ministry and counsellors who took the time to listen.

In particular, I would like to thank my supervisors, Olga Vilela, Faiza Azam and Diego Miranda, because without them this work would not have been possible. Each one played a unique role, bringing experience in the field, discussing how the CAMS system works and always accompanying the work in progress.

Finally, I would like to thank the friends I met during the Energy Engineering course. To each one who, together with me, spent days and nights dedicated to the course and sharing the struggles and joys.

ABSTRACT

This study evaluates the Copernicus Atmosphere Monitoring Service (CAMS) gridded solar radiation model in Brazil, focusing on its application for spatiotemporal analyses. The research validates 19 years of data (2005–2023) of the CAMS estimations against ground-based measurements from 11 stations dispersed throughout the country. Beyond pointwise comparisons, the work explores the model's ability to represent geographical patterns through the generation of monthly solar radiation anomaly and trend maps. The methodology employed included bilinear interpolation to align gridded data with station coordinates, calculation of statistical metrics, and seasonal analysis. The resulting maps revealed spatial variations linked to climatic phenomena, underscoring CAMS' utility for regional-scale studies. The conclusion emphasises the potential of CAMS as a promising tool for solar radiation mapping, acknowledging the challenges in fully representing local conditions. The approach demonstrates the potential of gridded models to complement in situ measurements, particularly in regions with limited data availability.

Keywords: Solar radiation; CAMS; gridded maps; validation; Brazil.

RESUMO

Este estudo avalia o modelo de radiação solar em grade do Copernicus Atmosphere Monitoring Service (CAMS) no Brasil, com foco em sua aplicação para análises espaço-temporais. A pesquisa valida 19 anos de dados (2005-2023) das estimativas do CAMS contra medições terrestres de 11 estações dispersas pelo país. Para além das comparações pontuais, o trabalho explora a capacidade do modelo para representar padrões geográficos através da geração de mapas mensais de anomalias e tendências da radiação solar. A metodologia utilizada incluiu a interpolação bilinear para alinhar os dados da grelha com as coordenadas das estações, o cálculo de métricas estatísticas e a análise sazonal. Os mapas resultantes revelaram variações espaciais ligadas a fenómenos climáticos, sublinhando a utilidade do CAMS para estudos à escala regional. A conclusão sublinha o potencial do CAMS como uma ferramenta promissora para a cartografia da radiação solar, reconhecendo os desafios na representação completa das condições locais. A abordagem demonstra o potencial dos modelos em grelha para complementar as medições in situ, particularmente em regiões com disponibilidade limitada de dados.

Palavras-chave: Radiação solar; CAMS; mapas em grade; validação; Brasil.

LIST OF FIGURES

LIST OF TABLES

LIST OF ABBREVIATIONS AND ACRONYMS

BNI	Beam Normal Irradiation
BHI	Beam Horizontal Irradiation
CAMS	Corpenicus Atmospheric Monitoring Service
DHI	Diffuse Horizontal Irradiation
DNI	Direct Normal Irradiation
GHI	Global Horizontal Irradiation
MBE	Mean Bias Error
RMSE	Root Mean Square Error
nMBE	Normalized Mean Bias Error
nRMSE	Normalized Root Mean Square Error

SUMMARY

1 INTRODUCTION

Solar radiation is one of the most abundant energy sources on the planet, and the use of solar energy systems is growing rapidly worldwide. This expansion has been fuelled by increased awareness of environmental sustainability and substantial reductions in the costs of solar photovoltaic systems. According to International Renewable Energy Agency Archives (IRENA), the average price of solar modules has dropped by over 87% since 2010, as seen in Figure 1, making solar energy more accessible and competitive compared to traditional energy sources. Solar photovoltaic generation reached 50.6 TWh (including centralized generation and micro and mini-distributed generation), marking a significant growth of 68.1% in the global scenario (BEN, 2024). This expansion plays a crucial role in the global energy transition, offering a cleaner and more sustainable alternative to traditional energy sources.

Figure 1 – PV Panel x Global Solar Capacity

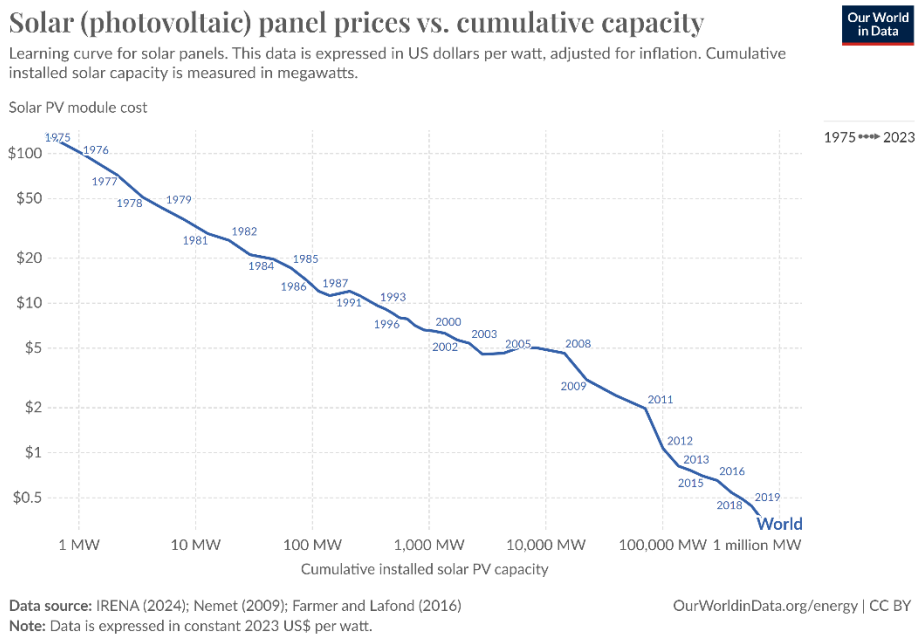

Fonte: Our World Data, 2025.

Energy from solar radiation can be used either as heat or electricity, depending on the application. While the variability and intermittency of solar resources present challenges for energy systems, the sustainability and affordability of solar photovoltaic equipment have encouraged investments in technologies that enhance energy storage

and grid integration (Lund, 2005). This affordability has also spurred innovations in monitoring and prediction systems, improving the reliability of solar power generation. Fluctuations in solar radiation over time can be attributed to meteorological factors such as cloud cover, aerosols and water vapor, and other influences, including human activity and natural phenomena (Iqbal, 2012). Therefore, a detailed study of solar radiation is essential for assessing the solar potential of various regions and for estimating radiation over days, months and years (Notton and Voyant, 2018).

The proposed work focuses on the evaluation of an extensive series of solar irradiance data offered by the Copernicus Atmosphere Monitoring Service (CAMS) within its Radiation Service (CRS). CRS contains 19 years of data, covering Africa, Europe, and parts of South America and Asia. This data offers invaluable insights into the distribution and temporal variability of solar radiation, which are vital for applications in solar energy, urban planning, agriculture, and climate studies. Analysing this database involves verifying the accuracy and consistency of the measurements (Esposito et al., 2024). This study aims to validate the quality of CAMS gridded solar radiation data by comparing it with ground measurements taken across the observed areas in Brazil. The goal is to assess the reliability of this database and contribute to the information needed for the expansion of large-scale solar power plant projects.

In addition, the collected data will be used to conduct a comprehensive analysis of the progression of radiation levels in Brazil over the years. This analysis will focus on the percentage variation in radiation exposure and its geographic distribution across the country. By investigating historical data, we aim to identify regions that have experienced higher or lower levels of radiation over time, allowing us to identify areas that are more impacted by radiation exposure. This detailed analysis will help understand the trends and patterns of radiation across different regions of Brazil, similar to a solar atlas as the Atlas Brasileiro de Energia Solar (INPE, 2017). This analysis aligns with the broader context of global solar energy expansion, where decreasing costs of solar technology continue to amplify the need for reliable data to support planning and policy decisions.

2 CAMS AND CAMS GRIDDED SOLAR RADIATION

Copernicus Atmosphere Monitoring Service (CAMS) is part of the Europea's Earth observation services and provides consistent, quality-controlled information related to air pollution and health, solar energy, greenhouse gases and climate behaviour (CAMS, 2025). CAMS offers CRS as a supplementary service with solar radiation time series as its primary product which is widely used for energy systems analysis. In addition, it also provides gridded data for energy system analysis on a spatial scale. Time series in 1 min, 15 min, hourly and daily temporal resolution are calculated 'on-the-fly' on user request at the desired location using atmosphere information from Meteosat satellites. In addition to the standard access as single time series at the user's individual target location, a gridded dataset for land surfaces of Europe and Africa and parts of Asia is available. This is based on a retrieved collection of many time series in a 0.1° spatial grid and in 15 min temporal resolution which are re-structured to a gridded monthly data file in netCDF format. See Figure 2.

Figure 2 – The general principle of CRS gridded data

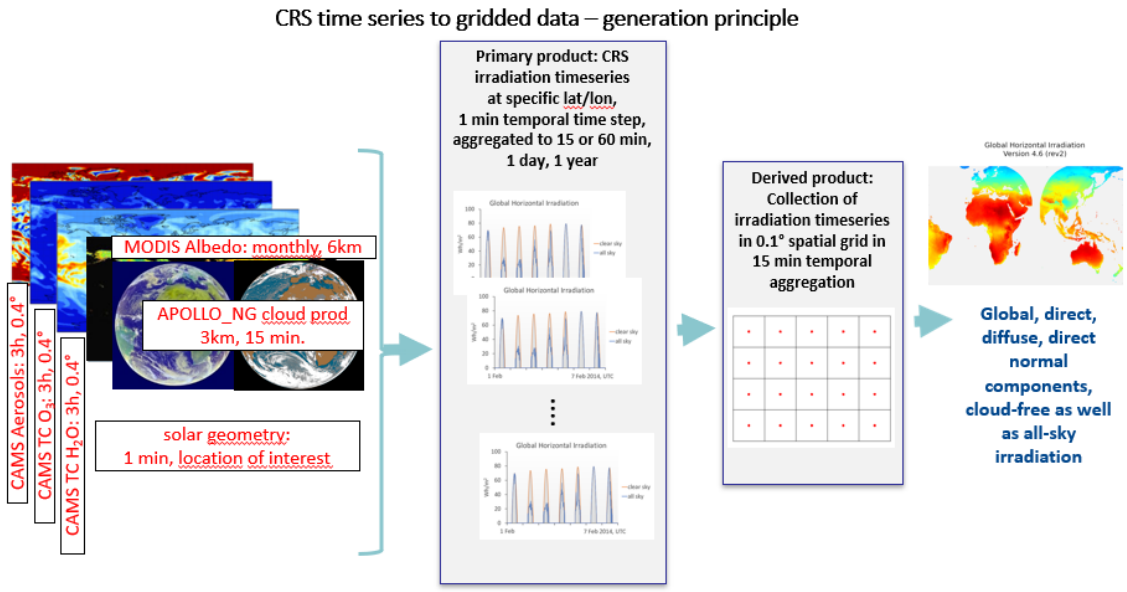

Source: (F. Azam, Personal Communication, 31.03.2025)

CAMS Gridded Solar Radiation (ECMWF, 2025) provides irradiance data from GHI (global horizontal irradiation), BNI (beam normal irradiation), BHI (beam horizontal irradiation) and DHI (diffuse horizontal irradiation). GHI is defined as the total solar

radiation received on a horizontal surface, incorporating both direct and diffuse components. BNI, on the other hand, refers to the direct solar radiation received perpendicularly to the Sun's rays, while BHI represents the direct component projected onto a horizontal plane. Finally, DHI accounts for the portion of solar radiation scattered by the atmosphere that reaches the surface from all directions (Santos, 2023).

These irradiance data are available for both clear and all-sky conditions on a latitude/longitude grid covering land surfaces. The clear sky model uses as input information on aerosols, ozone, water vapour and other atmospheric gases (Lefèvre et al., 2013; Gschwind et al., 2019) to calculate solar radiation values, while the all-sky model considers the interference of clouds in those values (Qu et al., 2017; CAMS, 2025). The dataset contains irradiation in Wh/m^2 with a time step of 15 minutes, ranging from January 2005 to December 2023.

The CAMS Gridded Solar Radiation product offers several advantages over the CAMS Time Series product, providing greater flexibility for a wide range of applications. The CAMS Time Series product delivers more detailed information at a single point and is at a higher temporal resolution than 15 min. However, it's important to note that all the detailed information provided by the CAMS Time Series product is derived from interpolation on the points between the satellite measurements temporal resolution and modelling (Schroedter-Homscheidt et al., 2021).

The gridded format product offers data points across a continuous spatial grid and enables users to apply their own interpolation models to fill in gaps or enhance the resolution of the data, even allowing the use of multi-source data for the modelling (Şen; Şahİn, 2001). Moreover, customised modelling, such as the use of advanced machine learning or physics-based models, can be applied to better understand the spatial relation of solar radiation in a certain area, increasing the accuracy of forecast models in the region, and even supporting more informed decisions in other sectors such as agriculture and environmental management (Vestnik, 2013).

3 METHODOLOGY

After downloading the CAMS data, the data were cut into a rectangular area encompassing the latitude and longitude points where Brazil is located to reduce the computational burden of the subsequent operations. The original dataset covered a global grid from -66º to 65º in both latitude and longitude, which was reduced to a regional subset from -36º to 10º latitude and -61º to -32º longitude. Subsequently, some data processing was performed, such as changing the units of the radiation values and adjusting the time step to match the observed values from each station.

The time-step adjustment was necessary because CAMS gridded data have a different temporal resolution compared to the another time-series. While the observational data and CAMS time-series are available at time interval of one minute resolution, the CAMS gridded dataset provided values at 15 minutes. To ensure consistency, the CAMS time series and the measured data were resampled to align with the timestamps of the gridded data, by computing the mean for each corresponding time step.

To compare the CAMS product with data from a ground-based station, a bilinear interpolation was performed using the latitude and longitude of the four surrounding points where the station is located on the map. This spatial interpolation produces a data series that matches the latitude and longitude of the measured station data. This allows the calculation and analysis of statistical measures such as Mean Bias Erros (MBE) (Equation 1), Root Mean Square Error (RMSE) (Equation 2) and Pearson Correlation Coefficient (Equation 3) (Cavalcanti, 2022). Where X is the average data while Y is the data to be evaluated, either CAMS gridded or time-series.

$$MBE = \overline{X} - \overline{Y} \tag{1}$$

$$RMSE = \sqrt{\frac{1}{n}\sum_{i=1}^{n}(x-y)^2} \tag{2}$$

$$\rho = \sqrt{\frac{cov(X,Y)}{cov(X,X)\cdot cov(Y,Y)}} \tag{3}$$

In addition, the percentage errors for the MBE and RMSE were also calculated from the average value of the measured data, these being the Normalized Mean Bias Errors (nMBE) (Equation 4) and the Normalized Root Mean Square Error (nRMSE) (Equation 5).

$$nMBE = \frac{MBE}{\overline{X}} \tag{4}$$

$$nRMSE = \frac{RMSE}{\overline{X}} \tag{5}$$

For a proper evaluation, the data were aggregated to different time steps and compared accordingly. In the end, the data were compared at 15-minute, daily, and monthly time steps. Each comparison involved contrasting the CAMS gridded data with ground measurements, as well as comparing the CAMS series to the same ground data.

Statistics are gathered for each year to obtain detailed information about the quality of CAMS data over time. This approach enables the determination of whether there is a tendency for CAMS data to align more closely with ground-based data over time. Furthermore, the data were separated to evaluate the influence of seasons in each location, and statistics were calculated for each season of the year. In parallel, CAMS time-series are evaluated to compare both time-series and the bilinear interpolation of the gridded dataset products. This comparison will highlight the differences between the bilinear interpolated data and the data processed by CAMS.

A multitude of sources were used in the collection of ground data, including the Sistema de Organização Nacional de Dados Ambientais (SONDA) from the INPE, the Baseline Surface Radiation Network (BSRN), and the International Energy Agency (IEA). In total, eleven stations were utilised, which are listed below in Table 1. The table also provides the following details: latitude, longitude, altitude, the period of the measured data and the average daily radiation of the measured series. The climates of each location in Köppen-Geiger classification are also provided, with information sourced from the Climate Change Knowledge Portal of the World Bank Group. The

spatial distribution of the stations can be observed in Figure 3, where they are indicated on the map.

Table 1 – Stations List

Station	Latitude	Longitude	Altitude	Daily Means	Period	Climate
Petrolina	-9.07	-40.32	387 m	5.51 kWh/m²	Mar2008 to Dec2020	Hot Semi-Arid
São Luiz	-2.59	-44.21	40 m	4.84 kWh/m²	Jan2007 to Apr2019	Tropical Savanna
São Martinho da Serra	-29.44	-53.82	489 m	4.79 kWh/m²	Apr2006 to Jun2017	Humid Subtropical
Ourinhos	-22.95	-49.89	446 m	4.80 kWh/m²	Feb2006 to Apr2019	Humid Subtropical
Brasília	-15.60	-47.71	1023 m	5.40 kWh/m²	Feb2006 to Apr2019	Tropical Savanna
Natal	-5.84	-35.21	58 m	5.80 kWh/m²	Jan2015 to Dec2019	Tropical Savanna
Cachoeira Paulista	-22.69	-45.01	574 m	4.93 kWh/m²	Jan2015 to Dec2019	Humid Subtropical
Florianópolis	-27.60	-48.52	31 m	4.27 kWh/m²	Sep2013 to Dec2022	Humid Subtropical
Patos	-7.01	-37.30	267 m	6.23 kWh/m²	Apr2012 to Dec2018	Hot Semi-Arid
Coremas	-7.02	-37.94	239 m	6,15 kWh/m²	Sep2012 to Aug2019	Tropical Savanna
São João do Rio do Peixe	-6.73	-38.45	251 m	6,28 kWh/m²	Sep2012 to Jan2019	Tropical Savanna

Source: Own Authorship, 2025

Figure 3 – Stations in Map

Source: Google My Maps, 2025

Following the collection of the measured data, it is imperative to conduct a rigorous testing process to ensure the exclusion of erroneous data from the evaluation. The quality control tests were conducted in accordance with the recommendations of the Baseline Surface Radiation Network (BSRN), thereby ensuring that the analysed solar radiation data met the established physical and statistical limits for reliable measurements. Initially, physically feasible limit tests were applied to verify whether the measured radiation values fell within expected ranges, considering the solar constant adjusted for the Earth-Sun distance and the solar zenith angle. Subsequently, the extremely rare limits test was conducted, imposing stricter constraints to identify potential systematic or instrumental errors.

Furthermore, consistency checks were performed among different radiation components. A pivotal test involved the verification of the ratio between the measured global radiation and the sum of direct and diffuse radiation, with adjustments made for the solar zenith angle (coherence test). This ratio was required to remain within a defined tolerance range, thereby ensuring consistency between different sensors. Another important validation step was assessing the ratio between diffuse and global radiation, which should not exceed expected threshold values under different solar

conditions. Furthermore, a tracker-off test is applied to evaluate when the tracker is not operating, which highly influences the measurements of diffuse and direct components of irradiance. Also, a clear sky filter and refining tests evaluating the first derivative of the solar irradiance time-series and its persistence are applied as additional tests. A detailed explanation of the quality checks used in this work is presented in Miranda et al. (2023). The sequence of these tests followed BSRN recommendations (BSRN, 2010), allowing for a progressive detection of errors and minimizing the impact of missing or invalid values on subsequent analyses.

As illustrated in Figures 4, 5 and 6, the percentage of anomalous values for each station in the GHI, DNI and DHI is demonstrated, respectively.

Figure 4 – GHI Quality Check

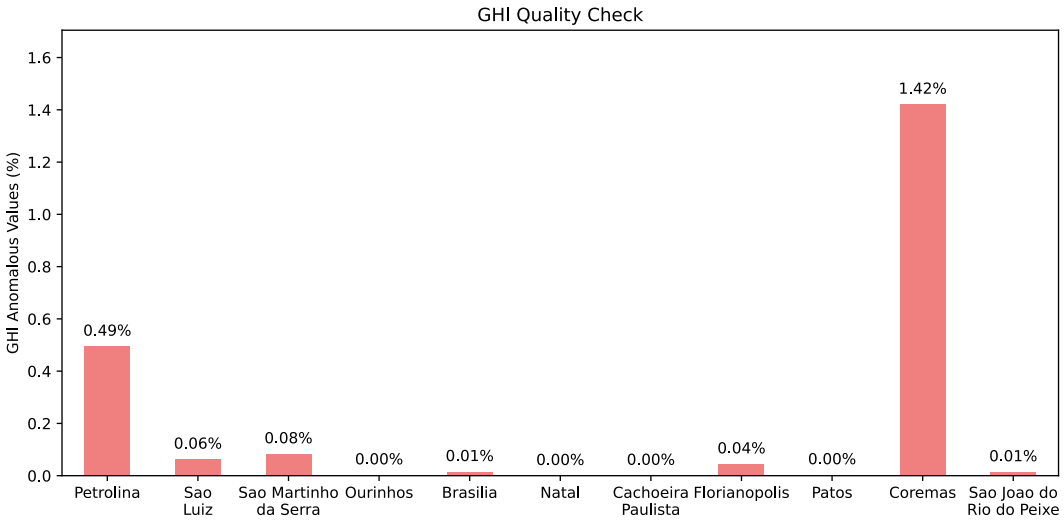

Source: Own Authorship, 2025

Figure 5 – DNI Quality Check

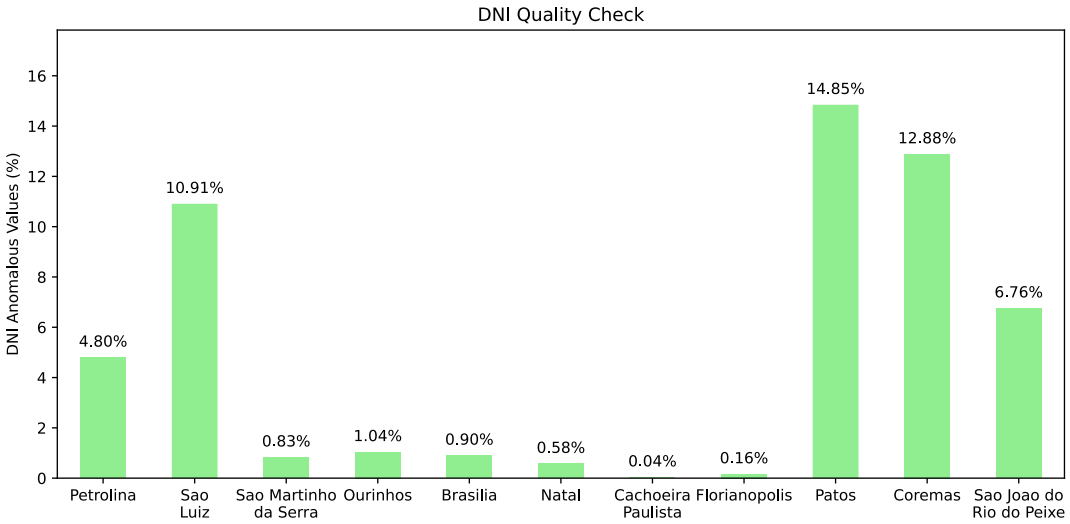

Source: Own Authorship, 2025

Figure 6 – DHI Quality Check

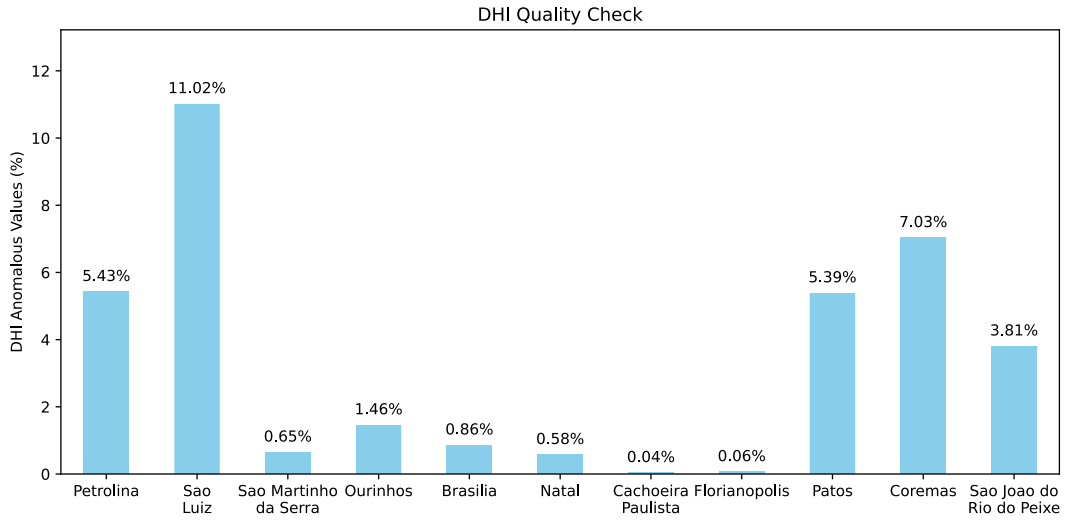

Source: Own Authorship, 2025

All the methodology described above, together with the anomaly map generation processes described below, can be seen in the flowchart shown in Figure 7, which presents the procedures followed on the analysis.

Figure 7 – Methodology Flowchart

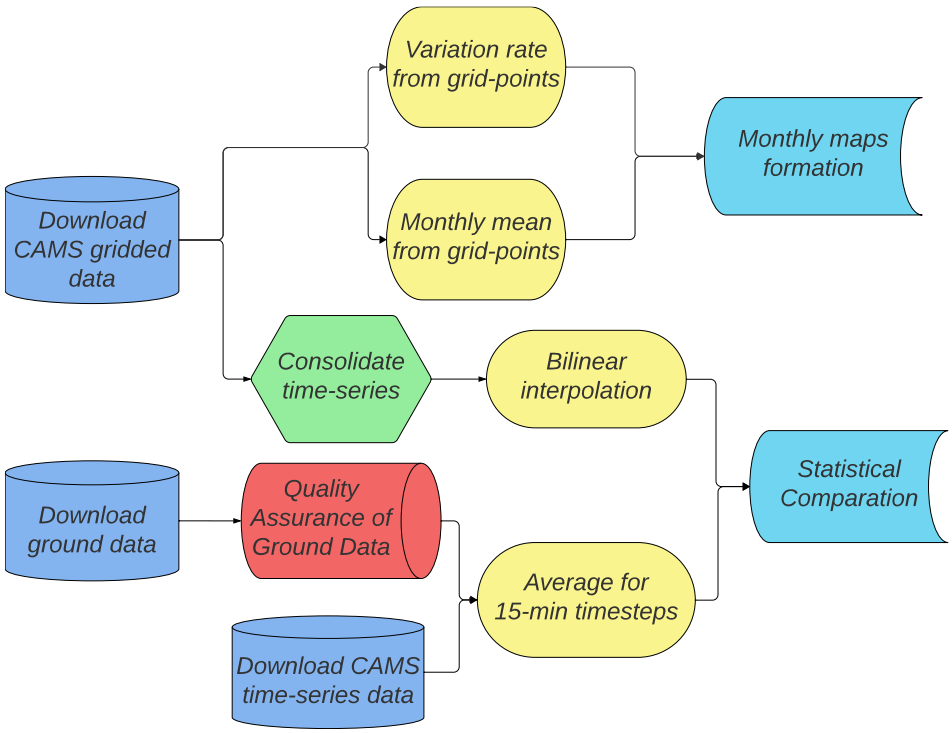

Source: Own Authorship, 2025

3.1 MAPS FORMATION

The validation of CAMS Gridded Radiation data facilitates the analysis of long-term variations in solar radiation across Brazil (INPE, 2017). The present study evaluates the percentage variation of radiation at each geographical grid point over time, thereby enabling the identification of spatial and temporal patterns in solar radiation anomalies.

To this end, the dataset, which consists of daily solar radiation values spanning a 19-year period, was processed to ensure spatial and temporal consistency. The data used for the map is the Global Horizontal Irradiance (GHI) structured on a geographical grid covering Brazil. The initial step entailed the computation of the historical monthly mean for each grid point. This was achieved by selecting all radiation values corresponding to a specific month across the 19-year period followed by calculating the average daily radiation for that month. This resulted in 12 reference datasets, one for each calendar month. The purpose of this approach was to create a baseline that accounts for seasonal variations, allowing for a more accurate assessment of deviations from expected radiation levels.

Once established, the historical means were then used to calculate the percentage anomaly for each month by comparing the observed radiation values with the corresponding historical mean. The anomaly was calculated using Equation 4:

$$Anomaly\ (\%) = 100\ \times \frac{Observed\ Radiation - Historical\ Mean}{Historical\ Mean} \quad (6)$$

This calculation was applied to every grid point, thereby generating a spatial matrix of percentage variation values. The resulting dataset was then visualised through the creation of anomaly maps, which facilitate an in-depth evaluation of solar radiation variability over time. These maps allow for the identification of recurring seasonal patterns, extreme variations, and potential long-term trends. By analysing different months and years, it is possible to detect spatial heterogeneities in solar radiation distribution and assess their potential implications for energy production and climate-related studies. An example of this analysis is presented in Figure 8, which illustrates the anomaly map for January 2005. The figure highlights regions with significant deviations from the historical mean, thereby demonstrating the applicability of the methodology in capturing spatial variations in solar radiation. The following maps in Figure 9 illustrate the monthly climatology with the solar radiation mean for each month of the year.

Figure 8 – Anomaly Map in January 2005

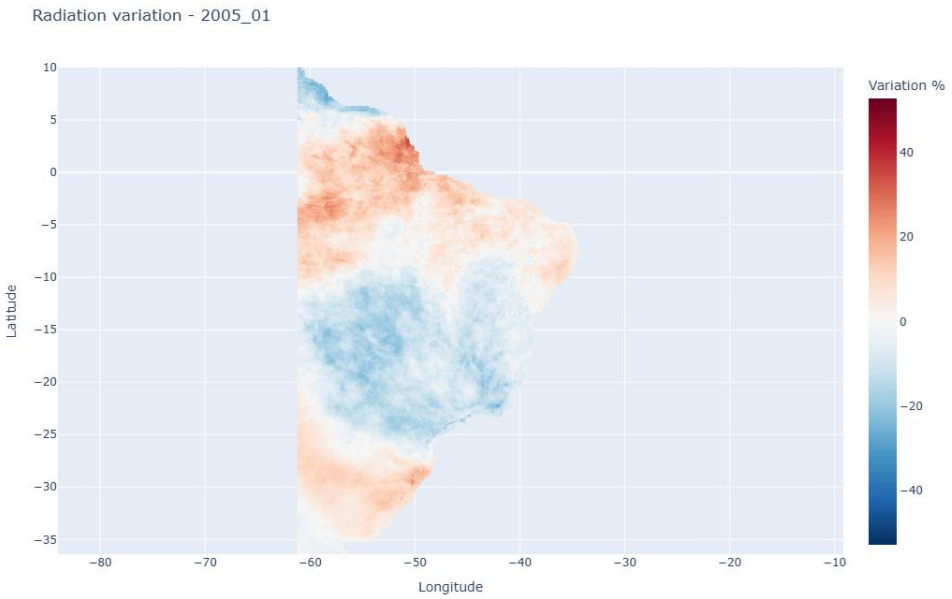

Fonte: Our World Data, 2025.

Figure 9 – Climatology Maps

a) January

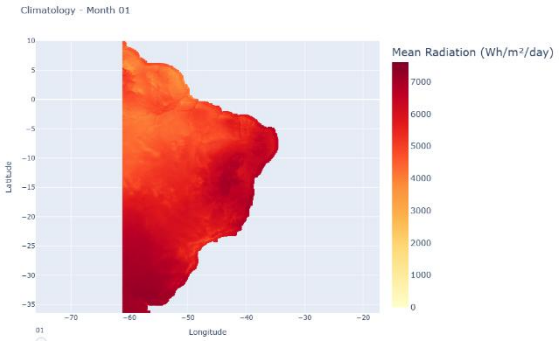

b) February

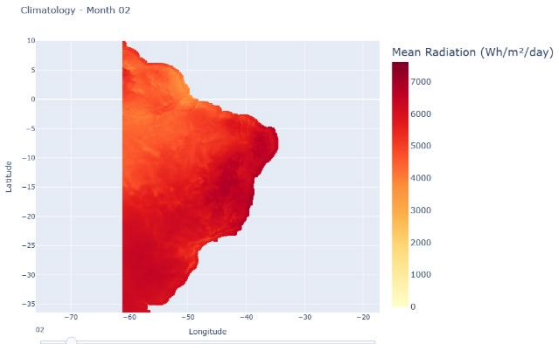

c) March

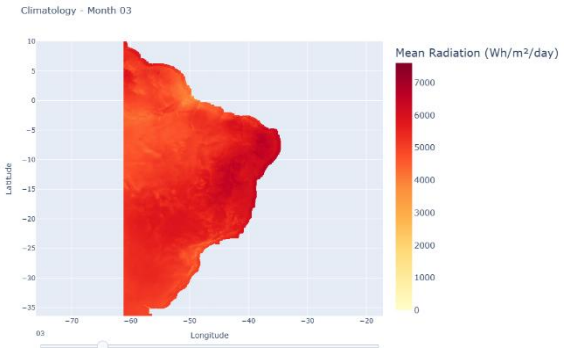

d) April

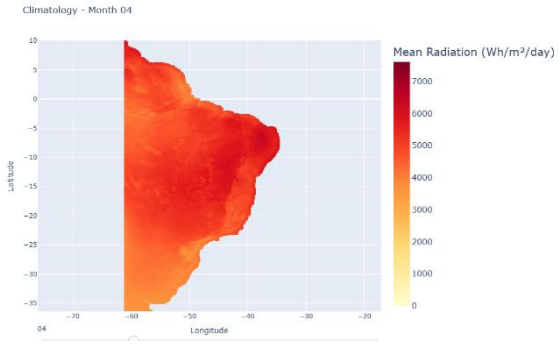

e) May

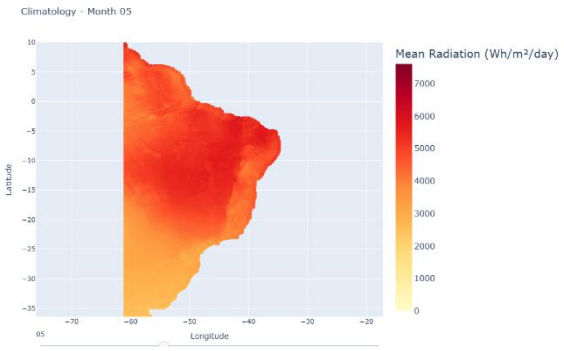

f) June

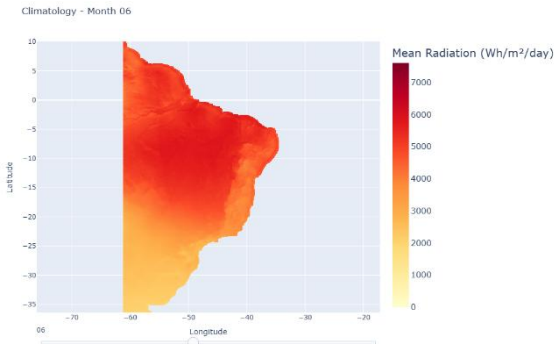

g) July

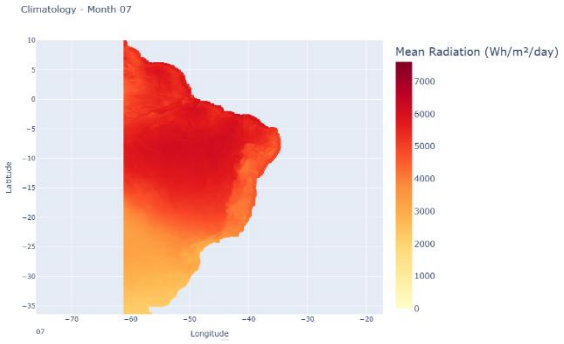

h) August

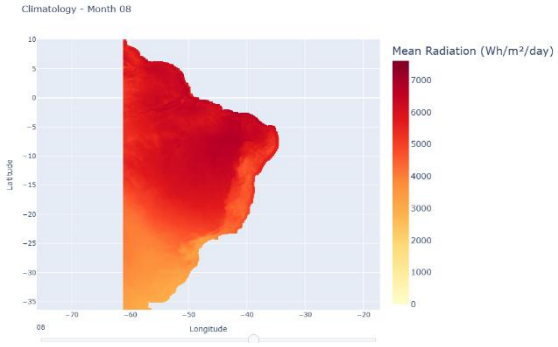

i) September

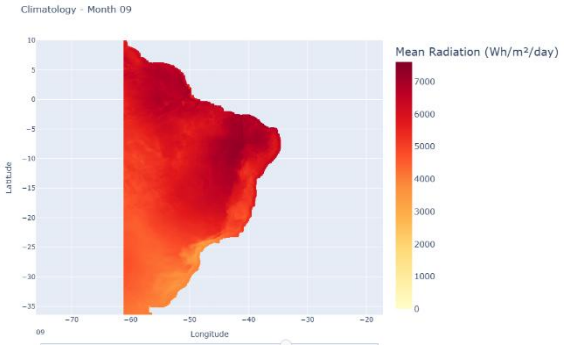

j) October

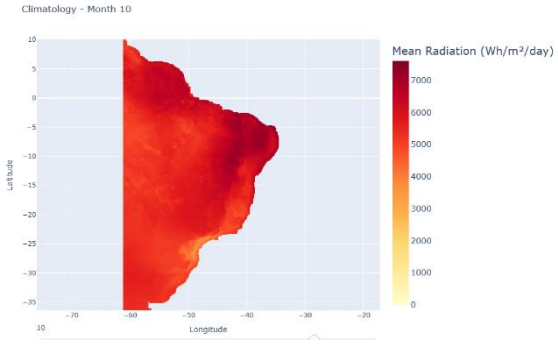

k) November

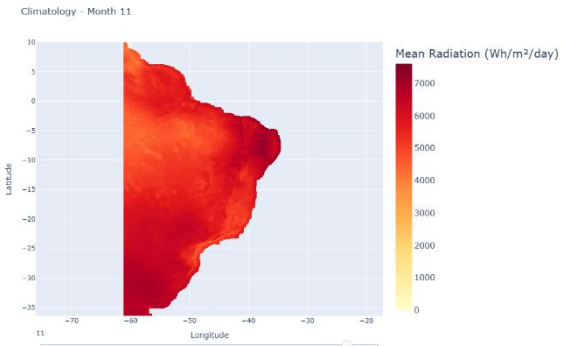

l) December

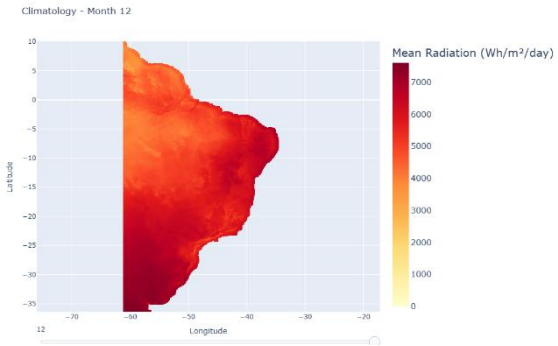

In addition, to observe more precisely the progression of solar radiation over the years for each region, the trend lines of each point were analysed separately for each

month of the year, observing the variation rate of these lines. This approach allows for a detailed analysis of how solar radiation changes every month, providing insights into seasonal variations and long-term trends (Pons and Ninyerola, 2008; Wilcox and Gueymard, 2010; Qi et al., 2024; Correa et al., 2024). By calculating the rate of change in Wh/year for each point, we can generate maps that visually represent the spatial and temporal distribution of these changes. The trend line for each point, derived from the monthly data, serves as a critical tool for understanding the dynamics of solar radiation over time. A case study near Petrolina can be seen in Figure 10, which shows the points representing each year of the series and the trend line generated in red.

Figure 10 – Petrolina Trend Line in January

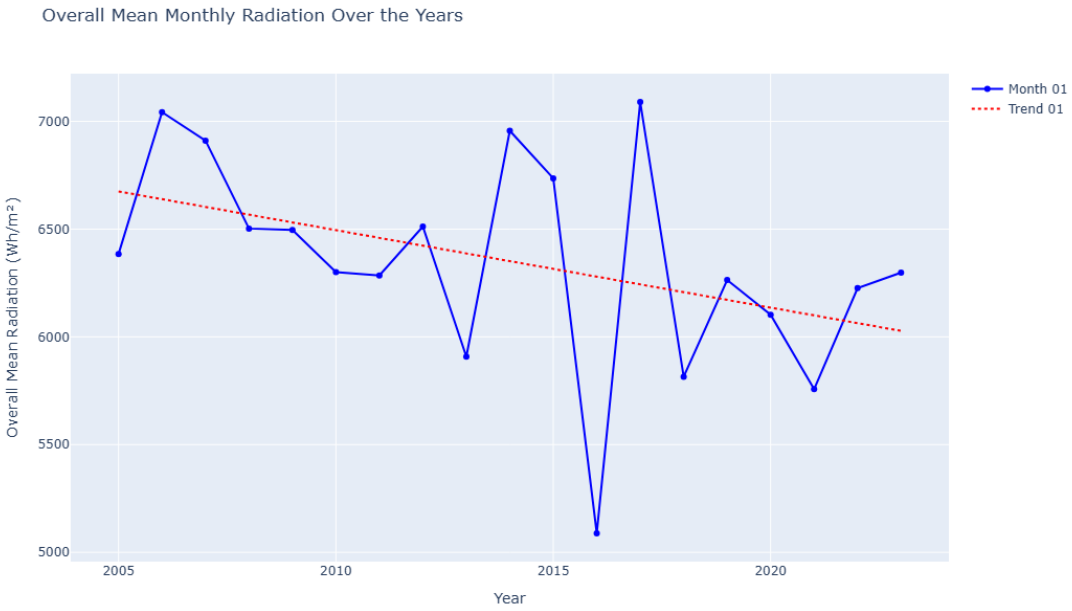

Fonte: Our World Data, 2025.

The generation of these maps, which incorporate the rate of change in Wh/year, provides a powerful visual representation of the data. Each map highlights the trends in solar radiation for specific months, allowing for a detailed examination of how these trends vary across different regions. By separating the data by month, we can better understand the seasonal influences on solar radiation and how these influences may be changing over time.

4 RESULTS

The statistical results obtained are presented in Appendix A. In general, CAMS model tends to overestimate solar radiation in comparison with ground-based measurements for the monthly statistics, as seen by the negative values of nMBE in Figure 11. However, an exception to this tendency is observed at the São Martinho da Serra station, where the distribution of positive and negative difference between model and measured data are more balanced, even presenting a closer agreement between the series at this location, as shown in nRMSE values in Figure 12. These results may be attributed to the influence of local atmospheric conditions, geographical features, or specific characteristics of the station's measurement setup, as the type of pyranometers used or some measuring errors that may passed through the quality check.

Figure 11 – GHI nMBE (%)

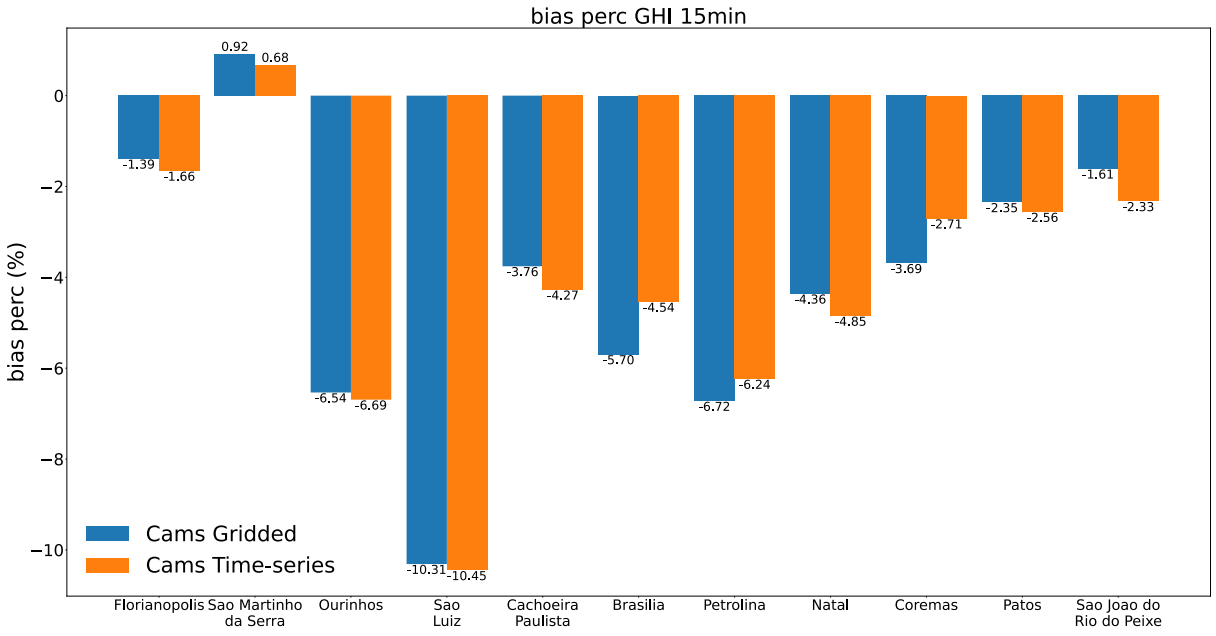

Source: Own Authorship, 2025

Figure 12 – GHI nRMSE (%)

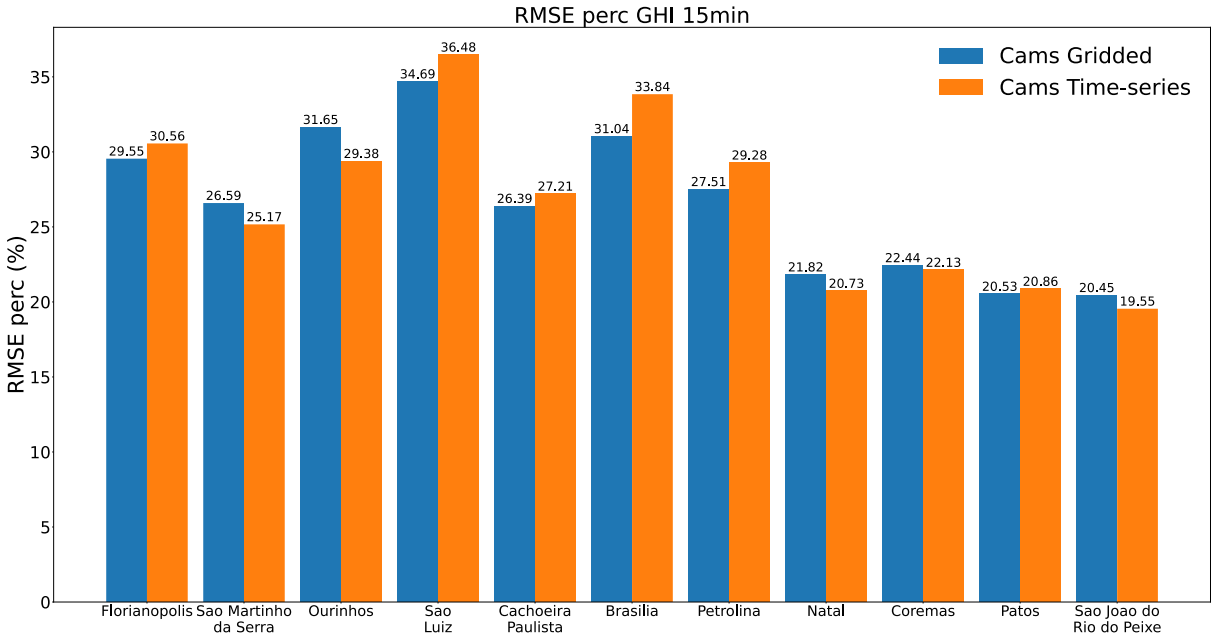

Source: Own Authorship, 2025

The sequence of bars has been sorted in such a way that the first bars have a lower average annual daily GHI radiation than the last ones, these values are shown in Table 1 with the stations list. The objective of this sorting is to ascertain the extent to which radiation levels and the presence of clouds throughout the year affect the performance of the CAMS models.

Moreover, a comparative analysis of the various radiation measurements reveals that the GHI model exhibits closer proximity to the measured values, with an nRMSE of approximately 30%, as opposed to the DNI and DHI models, seen in Figures 13 and 14 respectively, which demonstrate an approximate error of 50%, revealing how GHI models from CAMS have a better accuracy. Notably, certain stations have exhibited a higher degree of variability in their errors comparison between radiations, an example being the Ourinhos station, which exhibits an RMSE of 80% in the DNI model. Moreover, the values of the nMBE for the DNI and DHI are shown in Figures 15 and 16, respectively.

Figure 13 – DHI nRMSE (%)

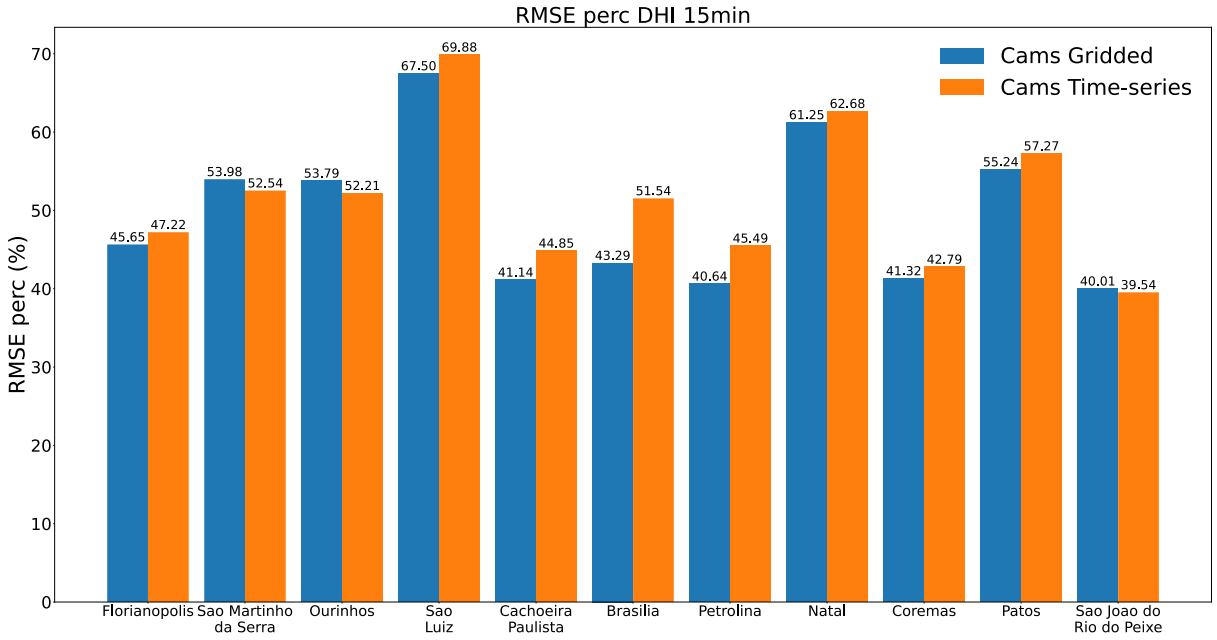

Source: Own Authorship, 2025

Figure 14 – DNI nRMSE (%)

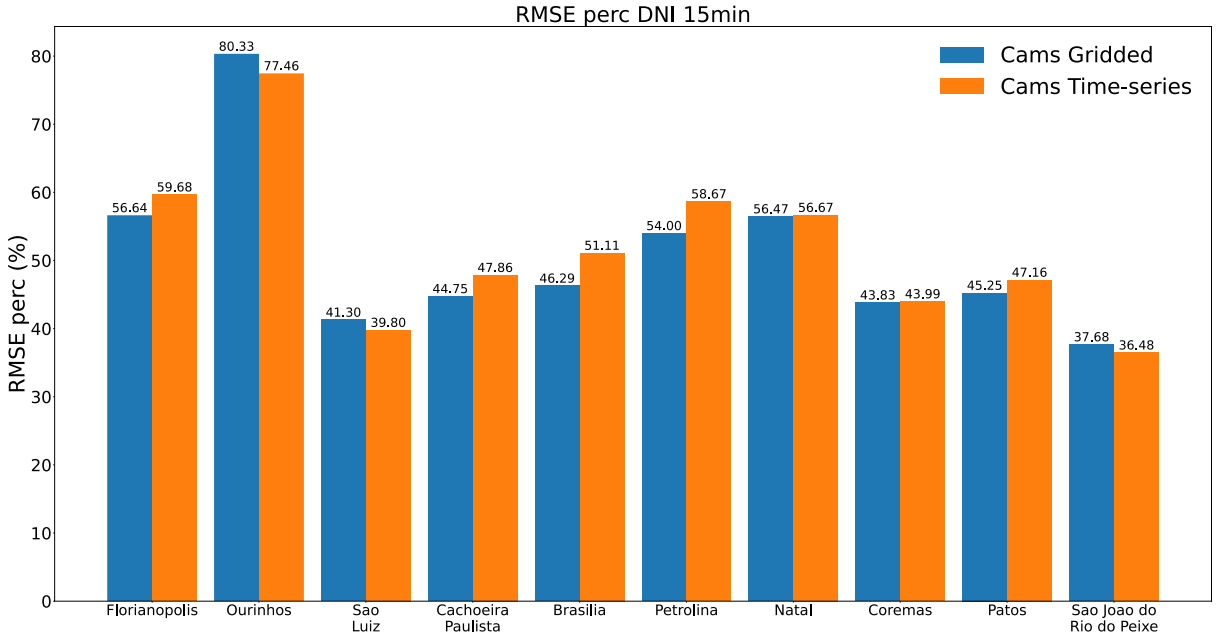

Source: Own Authorship, 2025

Figure 15 – DHI nMBE (%)

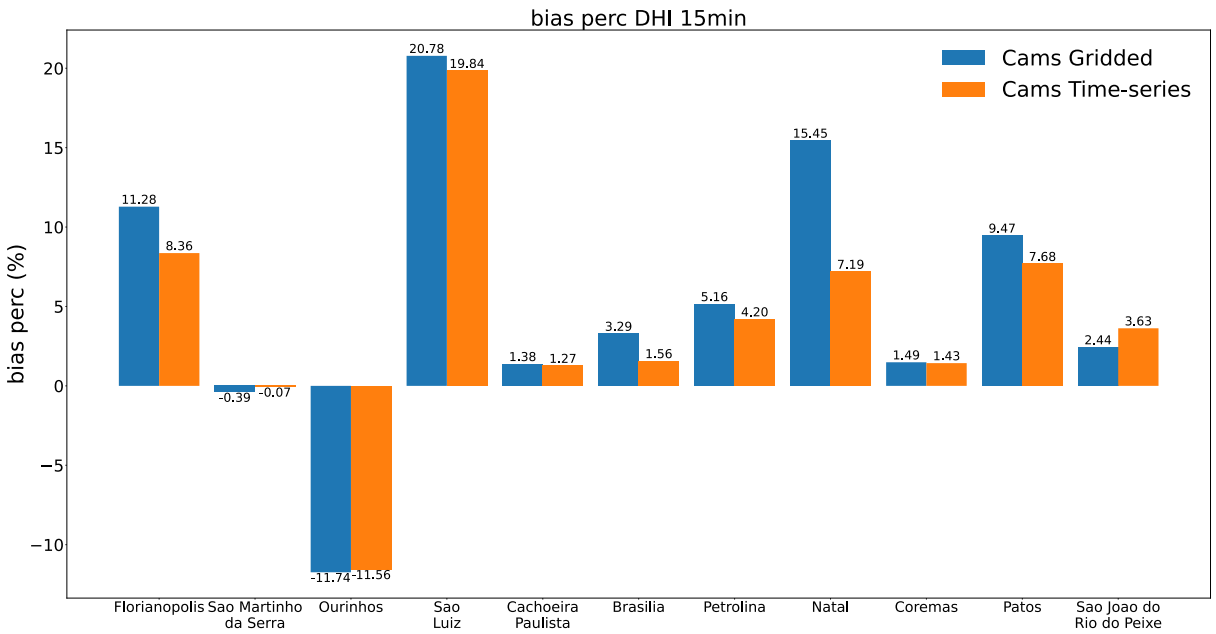

Source: Own Authorship, 2025

Figure 16 – DNI nMBE (%)

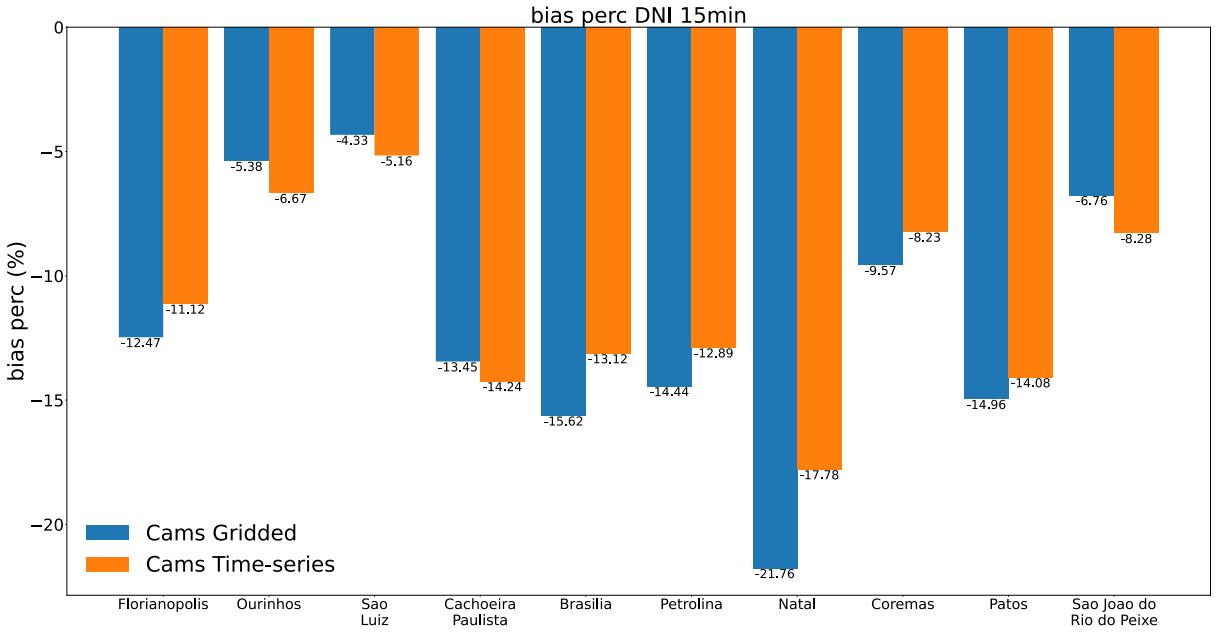

Source: Own Authorship, 2025

An essential aspect of this study is the comparison between CAMS Gridded radiation data, processed using bilinear interpolation (BI), and the CAMS time series, which provides point-specific values. Despite bilinear interpolation being a relatively

simple method for spatial estimation, the overall nRMSE results show a general approximation between CAMS Gridded (BI) and CAMS time series data.

Given the influence of bilinear interpolation on the results, it is important to emphasize that the comparison performed here involves CAMS Gridded data interpolated to the exact coordinates of the ground stations, rather than raw grid values. Thus, interpolation errors should be considered when using the CAMS Gridded Radiation for a specific point time-series.

A seasonal variation is observed across the graphs, with the lowest values occurring at the end of winter and the highest around the middle of summer and the beginning of autumn. One example is demonstrated in Figure 17, which presents a case study of Petrolina station, the blue bars denote the winter months, while the yellow bars represent the summer months. The summer season and beginning of autumn in most part of Brazil is marked by a transitional period for high cloud cover months, which directly impacts solar radiation levels (Sales et al., 2022). Figure 18 provides the percentage of time the sky is *clear*, *mostly clear*, or *partly cloudy* (i.e., less than *60%* of the sky is covered by clouds) according to the Weather Spark database, which is based on the MERRA-2 reanalysis model. Then, lower percentages indicate higher cloud cover which are likely higher in the period from November till beginning of March (summer season in Brazil including part of the autumn season).

Figure 17 – Monthly GHI nRMSE (%) - Petrolina

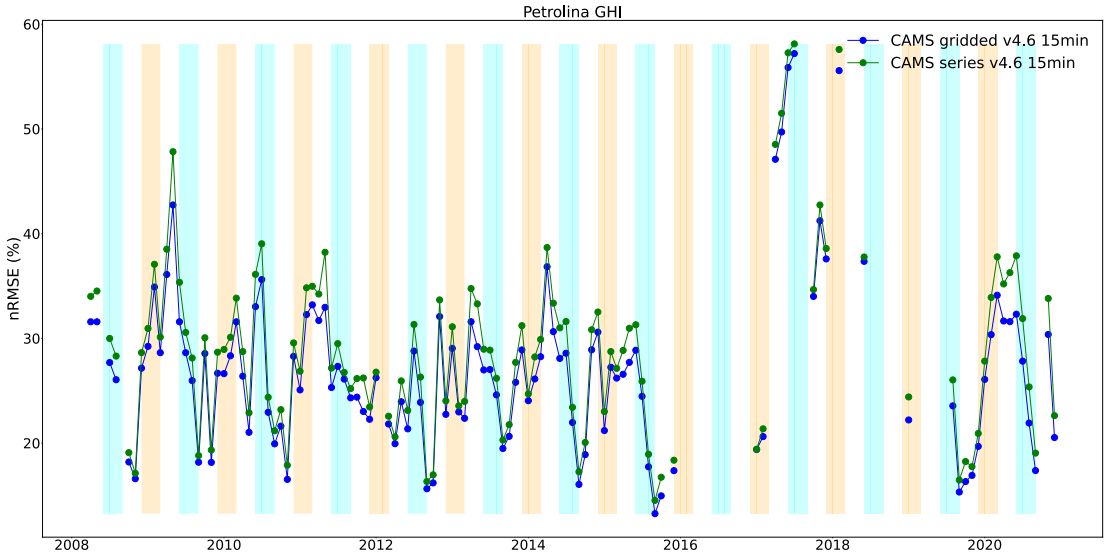

Source: Own Authorship, 2025

Figure 18 – Chances of Clearer Sky

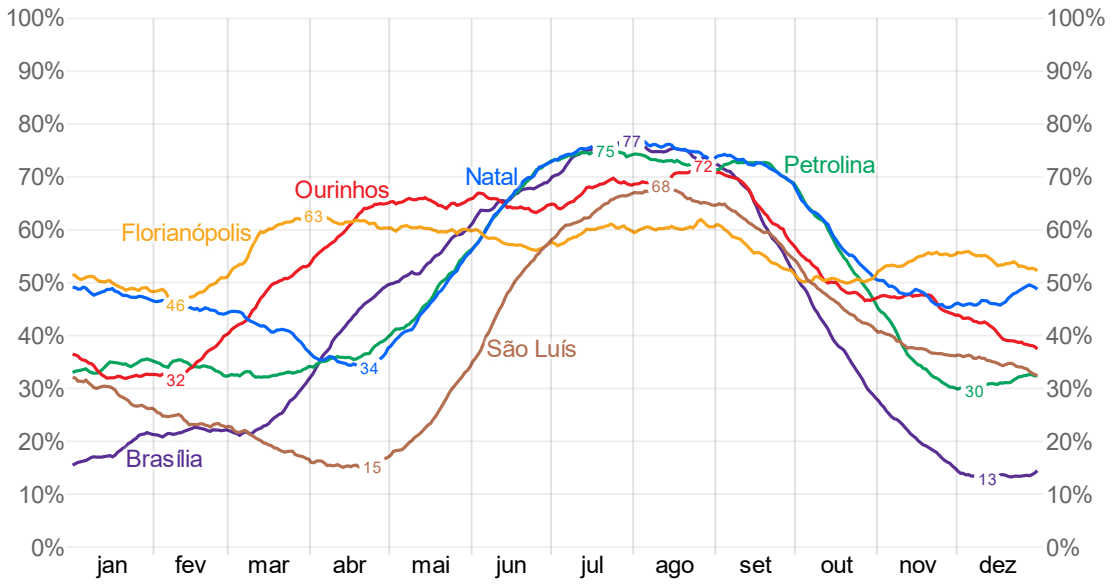

Source: Adapted from Weather Spark database, 2025

Additionally, to analyse the seasonal influence on CAMS errors in greater depth, the errors were aggregated by season. Figures 19 and 20 present the results for all stations, which reinforce the seasonal error pattern previously identified at the Petrolina station.

Figure 19 – Seasons nRMSE GHI CAMS gridded

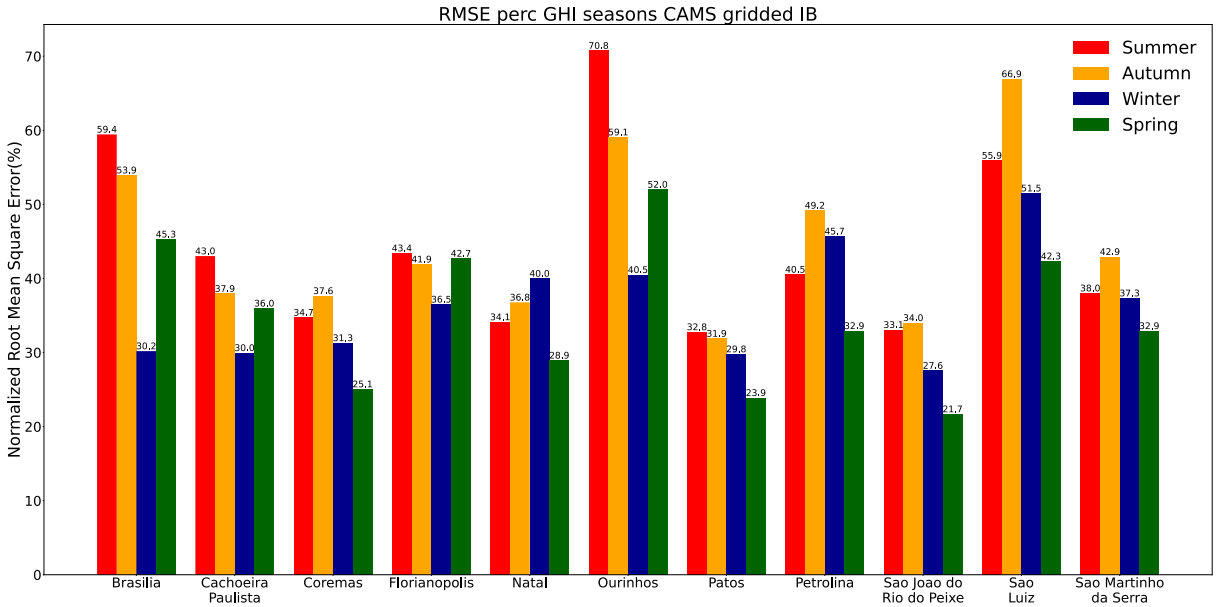

Source: Own Authorship, 2025

Figure 20 – Seasons nRMSE GHI CAMS time-series

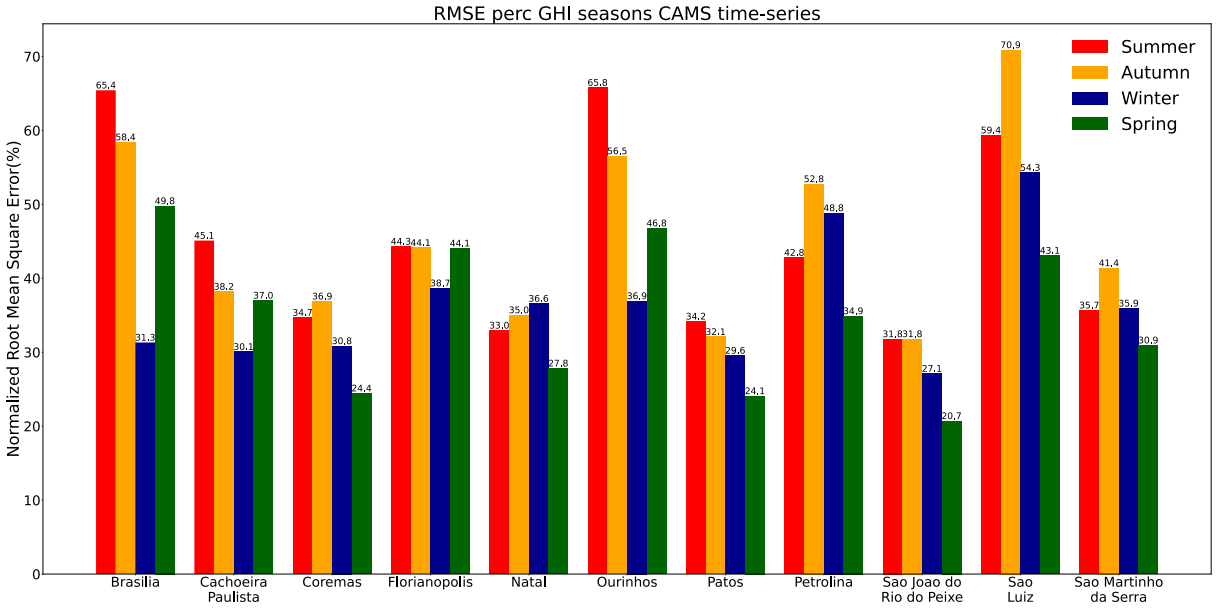

Source: Own Authorship, 2025

Moreover, the analysis of daily data reveals significantly smaller errors in comparison with those observed at other temporal resolutions, this is clear in the nRMSE graphics in Figure 21, 22 and 23 compared with 15 min resolution errors. This is an expected result that shows how short-term fluctuations in solar radiation tend to cancel each other out over the course of a day, thereby resulting in a more balanced representation of the overall radiation levels. The aggregation of 15-min values into daily means likely mitigates the impact of abrupt variations caused by transient weather conditions, such as passing clouds or sudden atmospheric changes (Yoshikane et al., 2023). This underscores the significance of temporal resolution in evaluating solar radiation models, as the choice of hourly or daily scale can influence the interpretation of errors and the assessment of model performance.

Figure 21 –nRMSE DHI daily

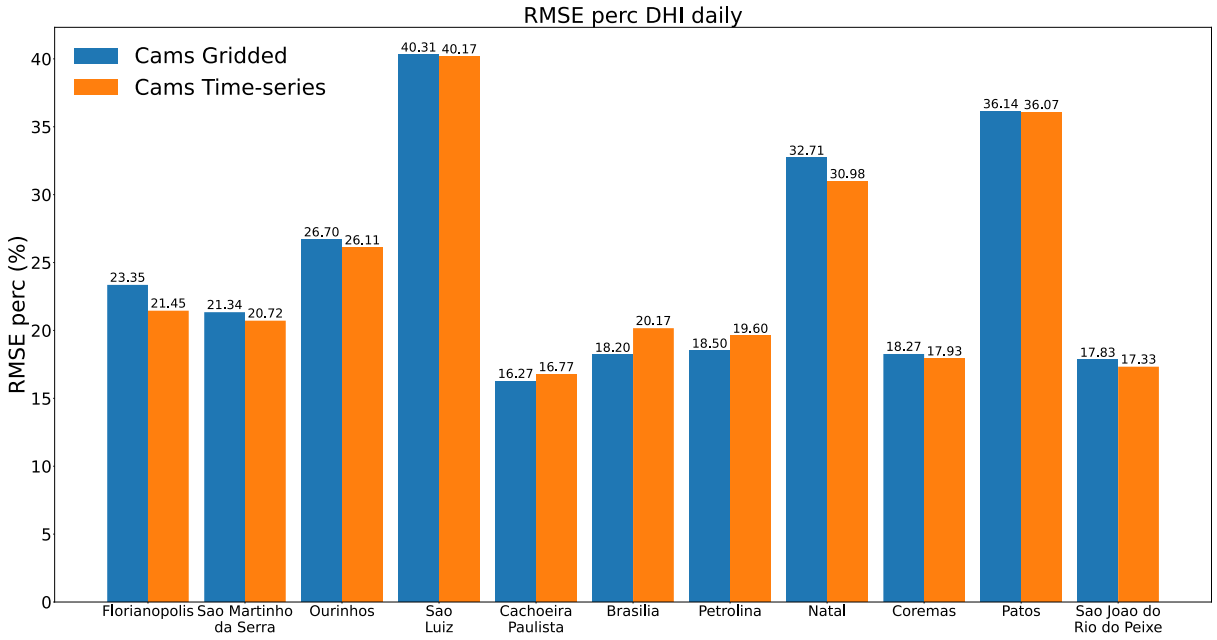

Source: Own Authorship, 2025

Figure 22 – nRMSE DNI daily

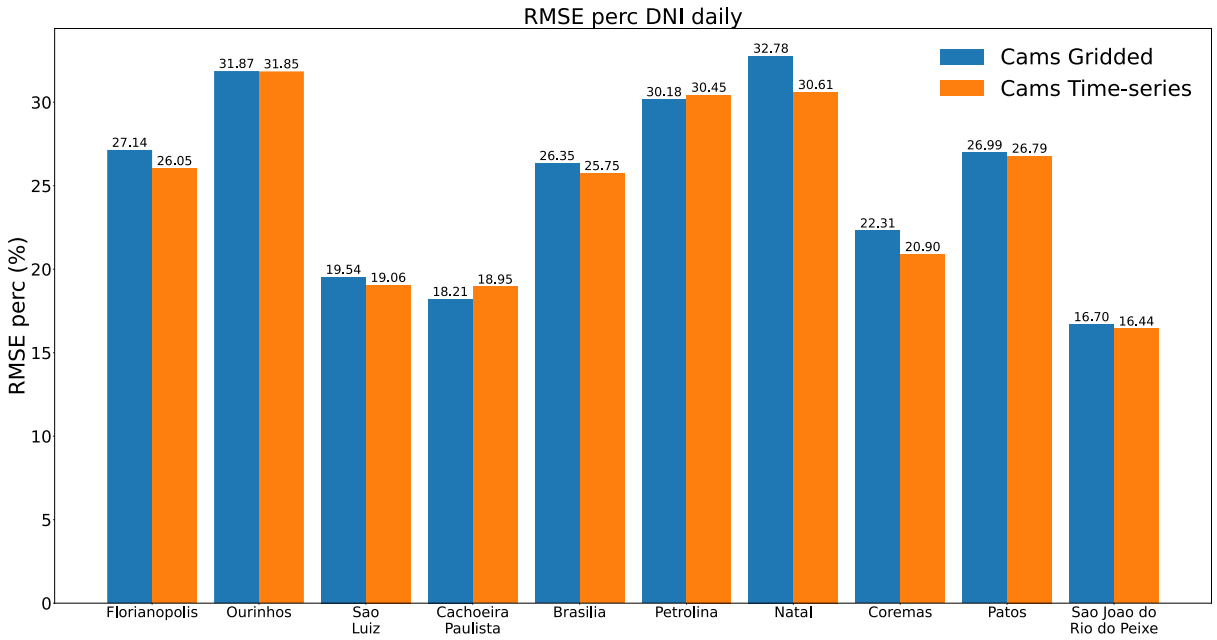

Source: Own Authorship, 2025

Figure 23 –nRMSE GHI daily

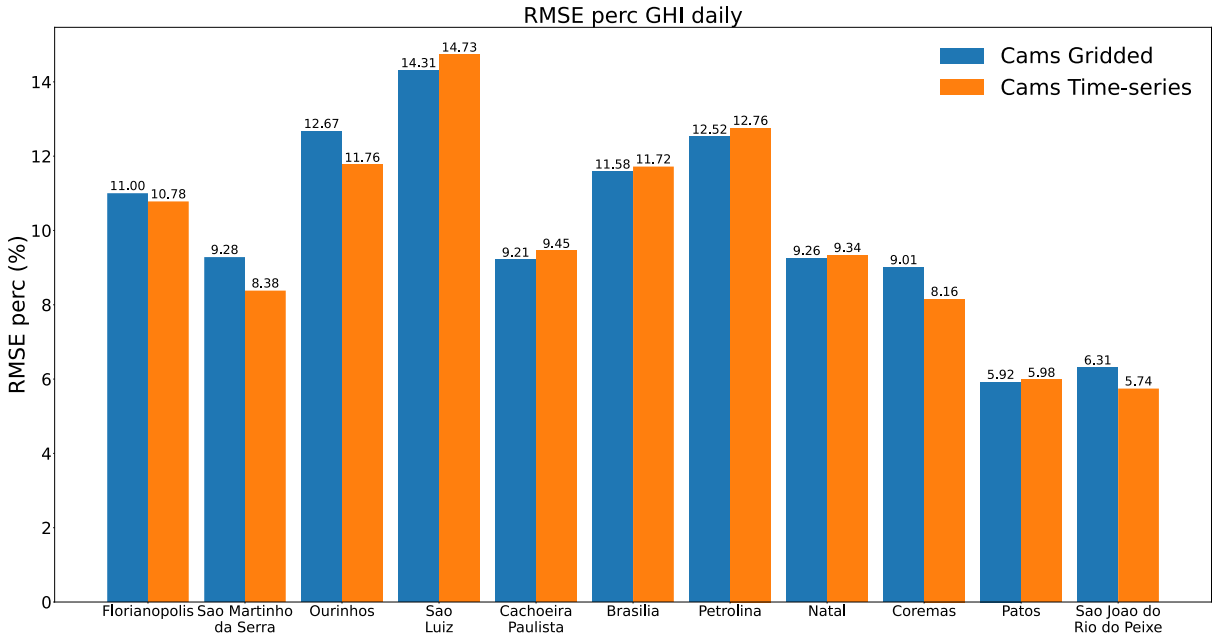

Source: Own Authorship, 2025

As the same event occurs on a monthly scale in Figures 24, 25 and 26, this highlights the importance of temporal resolution in the evaluation of solar radiation models, as the choice of 15-minute, daily and monthly scales can have an impact on the interpretation of errors and the assessment of model performance.

Figure 24 –nRMSE DHI monthly

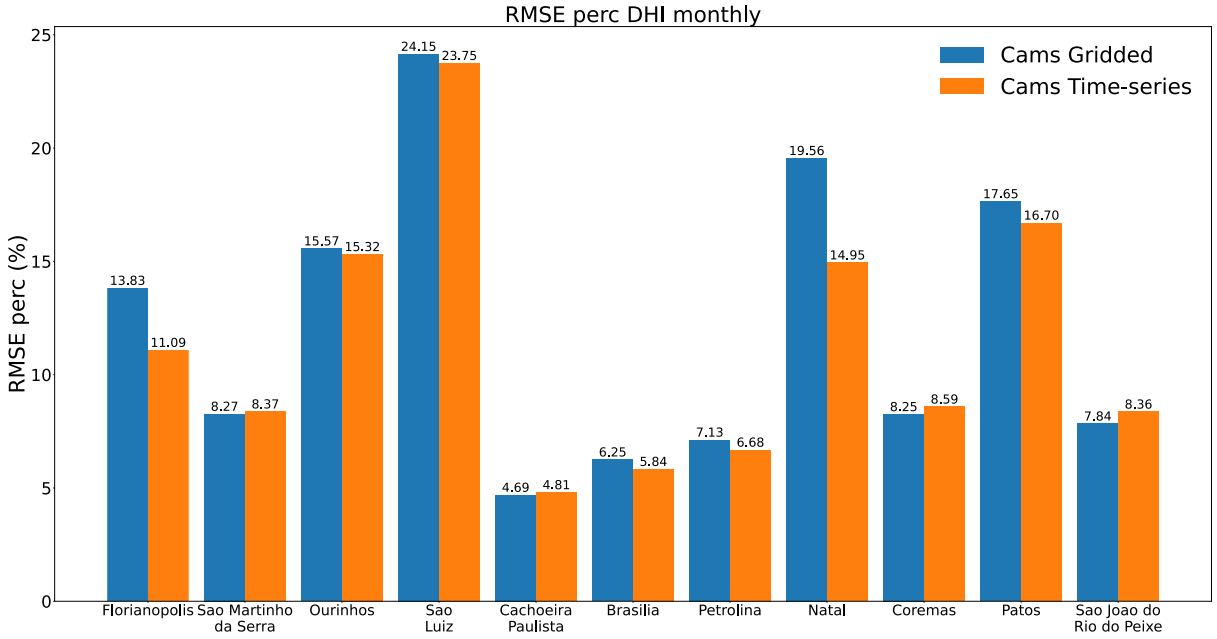

Source: Own Authorship, 2025

Figure 25 – nRMSE DNI monthly

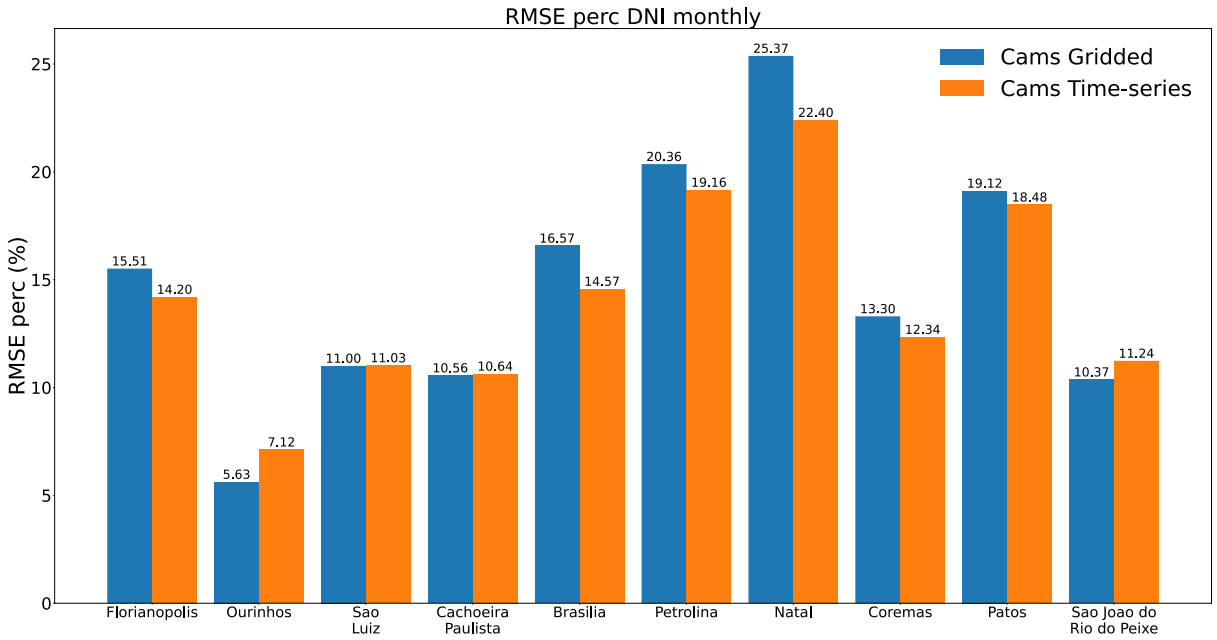

Source: Own Authorship, 2025

Figure 26 –nRMSE GHI monthly

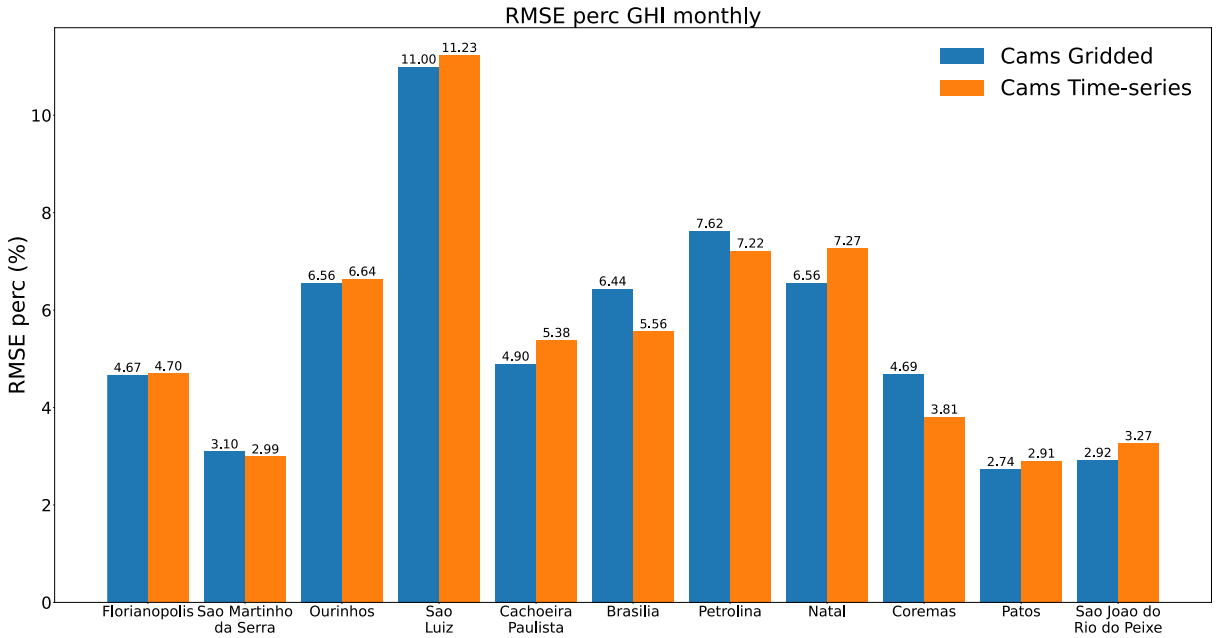

Source: Own Authorship, 2025

In evaluating the performance of bilinear interpolated CAMS Gridded and CAMS Time Series in comparison to ground measurements, it was established that the results varied from station to station. In certain instances, CAMS Gridded demonstrated a

closer approximation to the observed data, while in other instances, CAMS Time Series exhibited superior accuracy. This discrepancy underscores the necessity of incorporating spatial interpolation methodologies when utilising CAMS Gridded data, given its susceptibility to the technique employed for deriving values at particular station coordinates. The potential contributions of variations in local atmospheric conditions, terrain characteristics and interpolation assumptions are emphasised by these findings, highlighting the need for careful selection of data sources according to the specific application.

4.1 RADIATION MAPS

All maps anomaly maps are accessible through Appendix B. Regarding the anomaly maps, when analysing the spatial distribution of the radiation over the years, it is observable how certain regions experienced more pronounced changes during certain months. In some cases, the changes in radiation were significant compared to the expected values for a given month, highlighting local variations rather than a uniform trend, possibly as result of meteorologic events in the area. It is possible to see the results maps for all Decembers in Figure 26.

Figure 27 - Anomaly Maps for December

a) December 2005

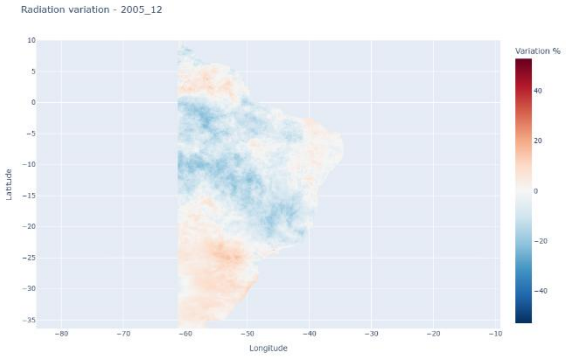

b) December 2006

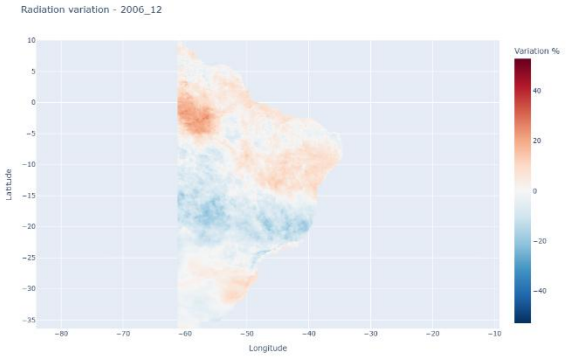

b) December 2007

b) December 2008

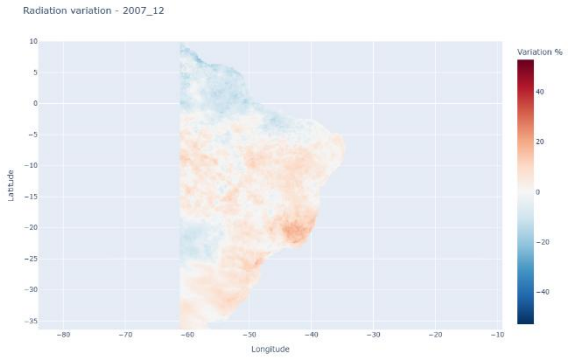

e) December 2009

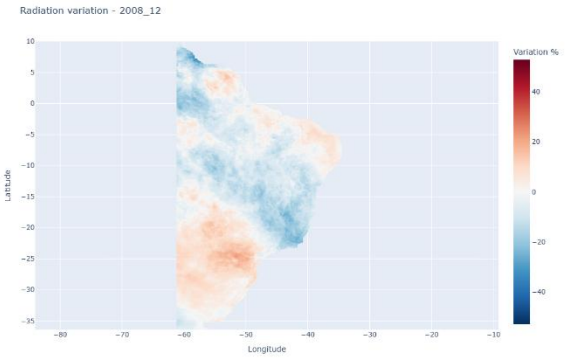

f) December 2010

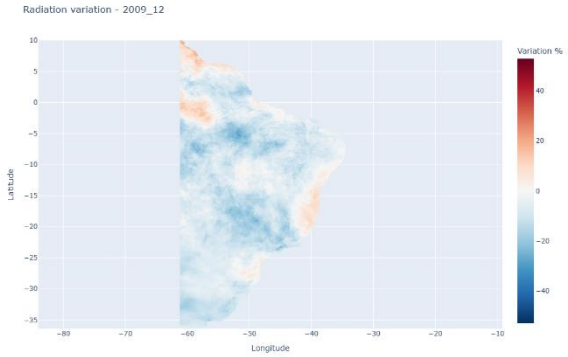

g) December 2011

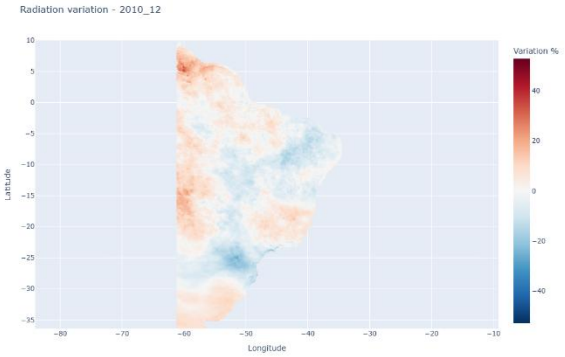

h) December 2012

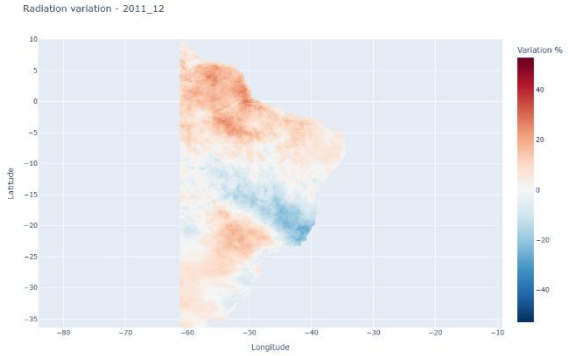

i) December 2013

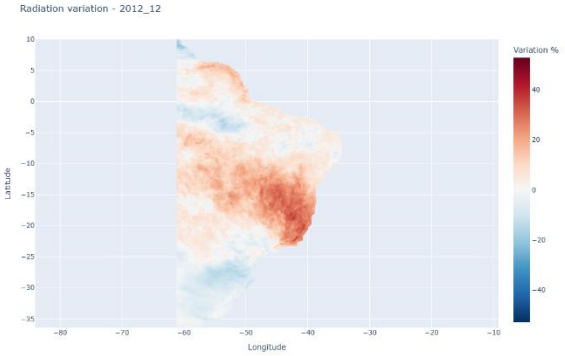

j) December 2014

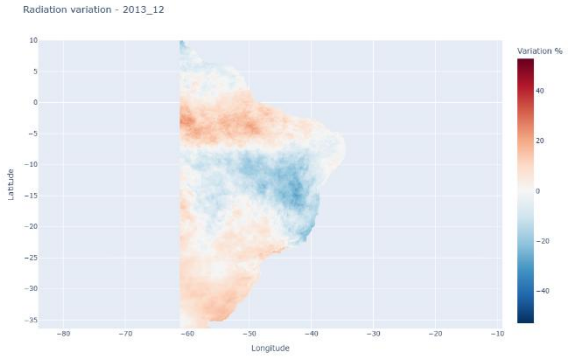

k) December 2015

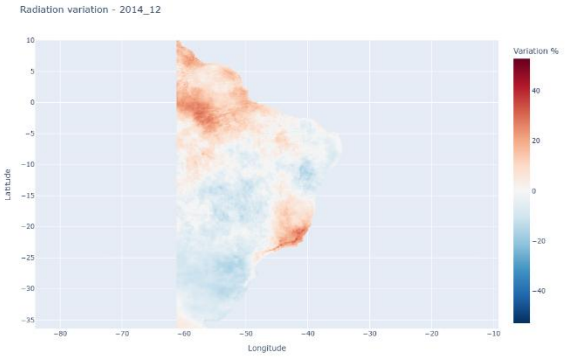

l) December 2016

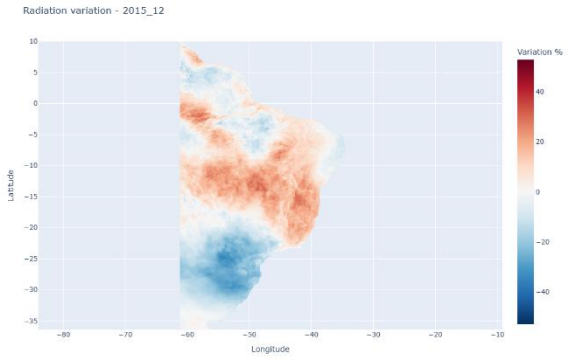

m) December 2017

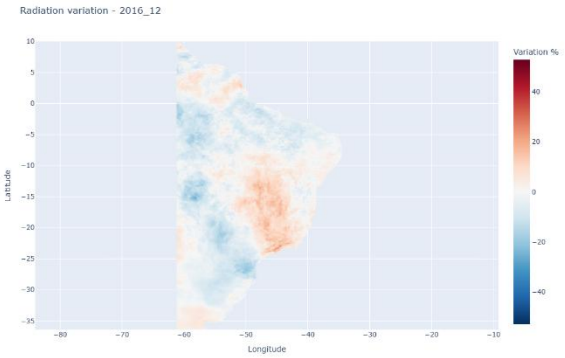

n) December 2018

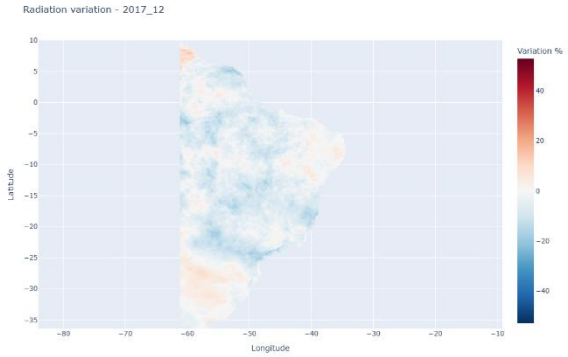

o) December 2019

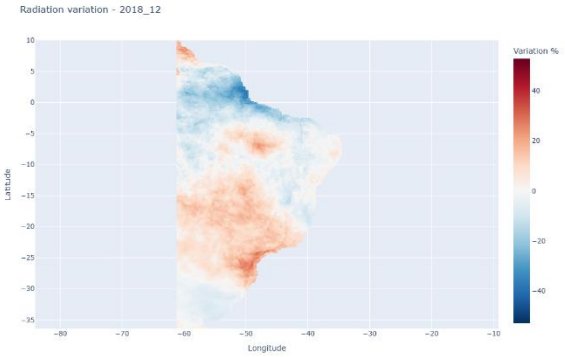

p) December 2020

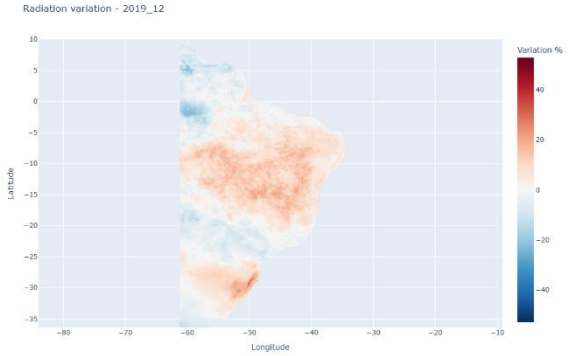

q) December 2021

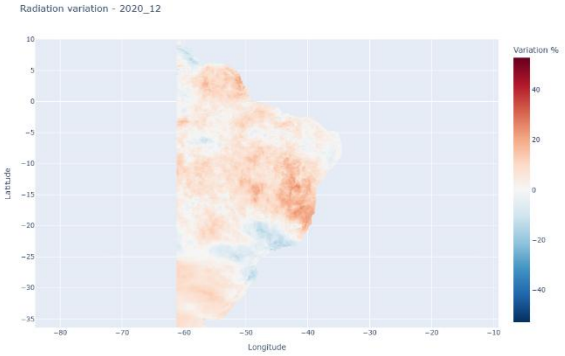

r) December 2022

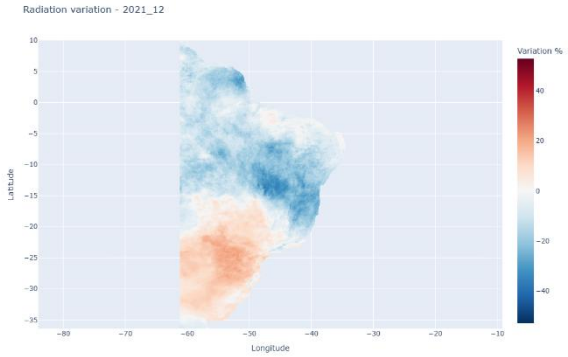

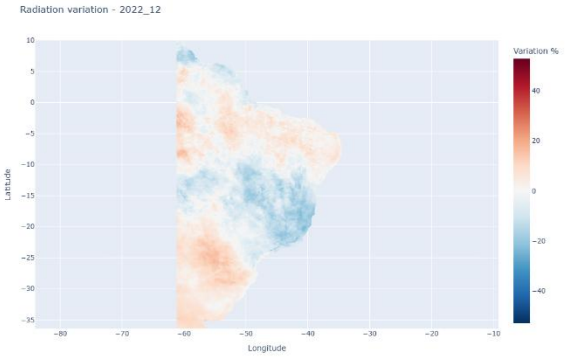

s) December 2023

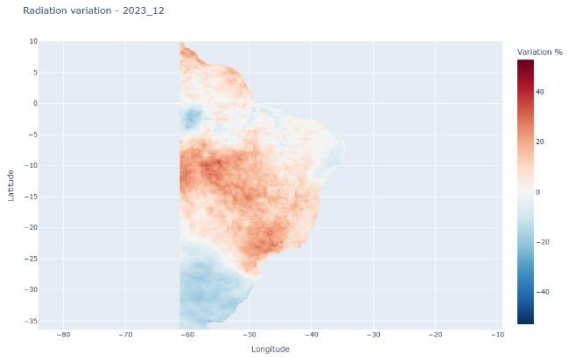

Source: Own Authorship, 2025

The analysis of solar radiation anomalies has revealed a distinct pattern associated with the ENSO (El Niño-Southern Oscillation) phases. El Niño is defined as the abnormal warming of the surface and subsurface waters of the equatorial Pacific Ocean, while La Niña is defined as their cooling (Oliveira, 2001). The El Niño meteorological phenomenon, when occurring in the northeast of Brazil, results in periods of drought, while in the south of the country there are periods of intense rainfall. Conversely, the La Niña phenomenon engenders an antithesis of this scenario (Freire et al., 2011).

During moderate to strong El Niño events, as in late 2015 and 2023, as marked in Figure 27, a discrepancy was observed between the central and northeastern regions, which exhibited positive anomaly, and the southern region, which displayed negative anomaly, shown in Figures 26k and 26s. This pattern is associated with the intensification of the Walker circulation during El Niño, which strengthens the convergence cell over the Pacific and amplifies the high-pressure system over northern and northeastern South America. The resulting subsidence of cold, dry air in these regions inhibits cloud formation, contributing to clearer skies and, consequently, increased solar radiation (Souza, 2002; Wang, 2002). In contrast, the southern region experiences enhanced moisture and rainfall during these periods, which leads to increased cloud cover and reduced radiation levels.

Figure 28 - Oceanic Niño Index (ONI)

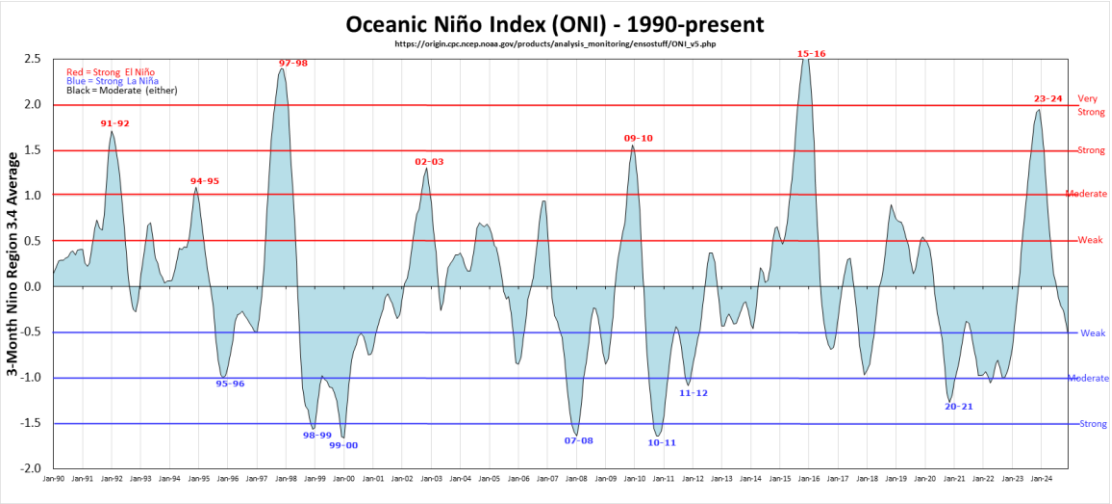

Source: GG Weather, accessed on 28 Mar 2025

In contrast, during a strong and moderate La Niña phase conditions, as in late 2010 and 2020 respectively, the variation in radiation tends to be more homogenous throughout the country, seen in Figures 26f and 26p thereby balancing out the difference that occurs in normal times between the north and south of Brazil.

These observations highlight the importance of taking ENSO phases into account when analysing long-term variations in solar radiation. The marked differences observed between El Niño and La Niña periods underscore the role of large-scale climatic phenomena in modulating solar energy variability. However, it is important to note that other climatological factors also play a significant role. For instance, although 2008 was marked by a strong La Niña event, it did not exhibit the same behaviour observed in other similar years, suggesting that ENSO alone cannot fully explain the observed variations. This underscores the crucial need for a comprehensive understanding of these variations by sectors that are dependent on solar radiation. The fluctuations in solar irradiance can directly impact resource management and operational efficiency in these sectors.

In addition to the anomaly maps, trend maps were generated to analyse the rate of change in solar radiation over the study period. A distinct spatial pattern emerges in the trend analysis, with a region of predominantly positive variation extending from the Southeast towards the Central and Northern areas of Brazil, exemplified by January in Figure 29. This suggests a systematic increase in solar radiation over time in these regions, which are also influenced by the large-scale atmospheric dynamics. One

potential factor influencing this pattern is the South Atlantic Convergence Zone (SACZ), a key meteorological system that impacts cloud cover and precipitation patterns over South America (Liebmann, 1999). Variations in the strength and persistence of the SACZ could influence the variability of solar radiation, leading to long-term changes observed in the trend maps.

Figure 29 - Trend Map for January

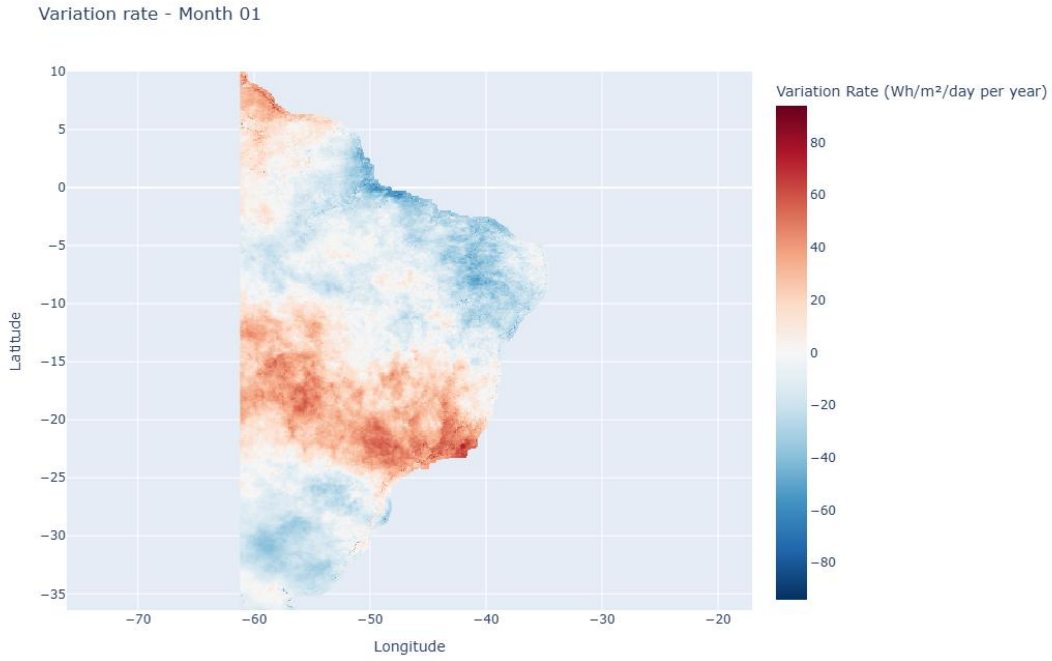

Source: Own Authorship, 2025

Furthermore, in Figure 30 there are all trend maps generated, each one, representing one month of the year. By interpreting these results, it becomes possible to assess how solar radiation trends might affect solar energy generation and regional climate dynamics. Understanding these trends is essential for both energy planning and climate studies, as they provide valuable information on the spatial and temporal distribution of solar resources across Brazil.

Figure 30 - Trends Maps

a) January

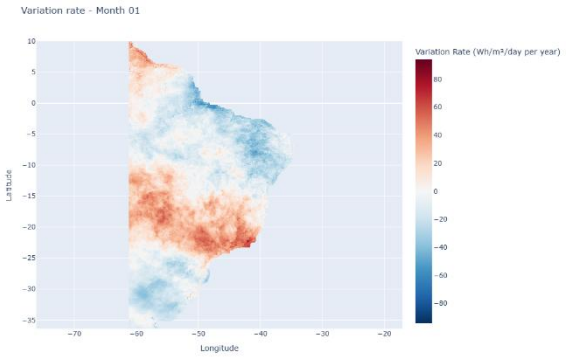

b) February

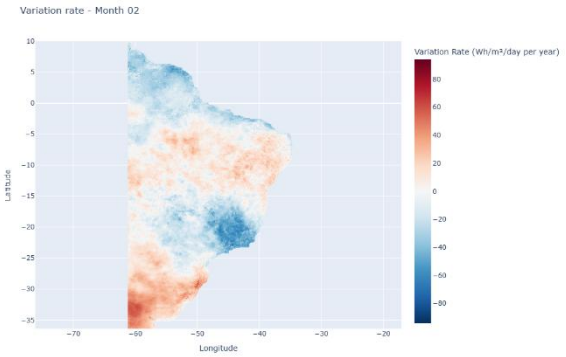

c) March

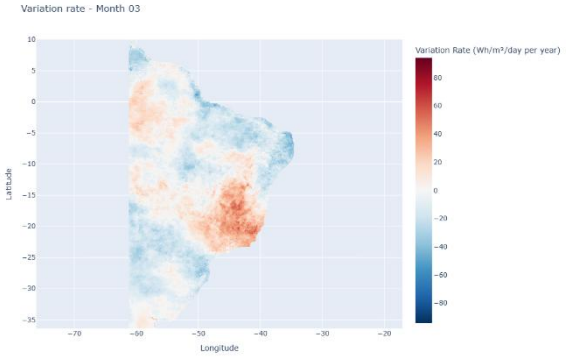

d) April

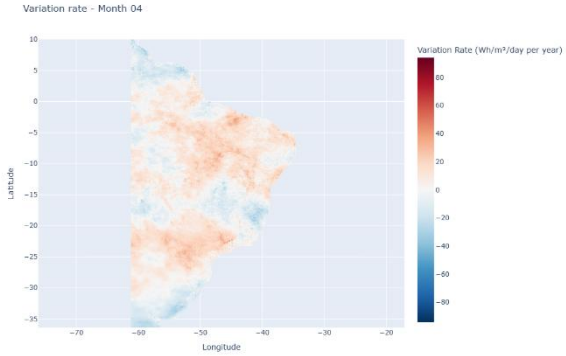

e) May

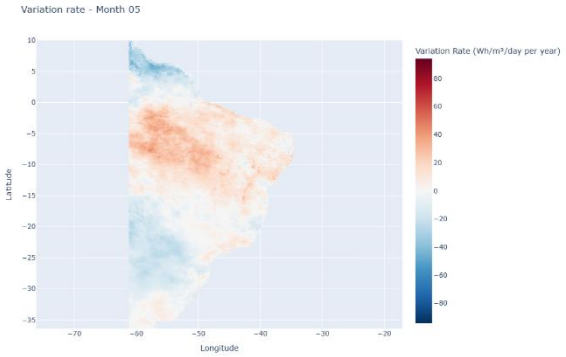

f) June

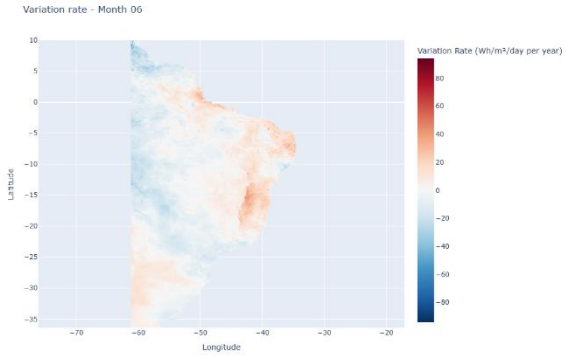

g) July

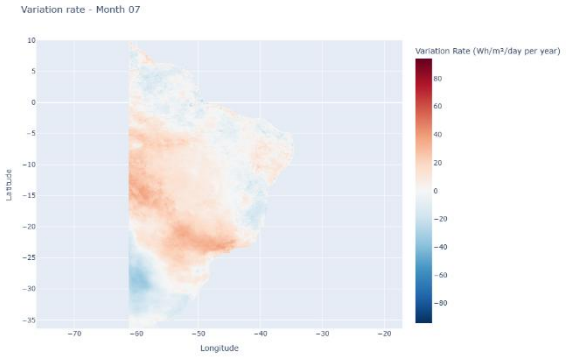

h) August

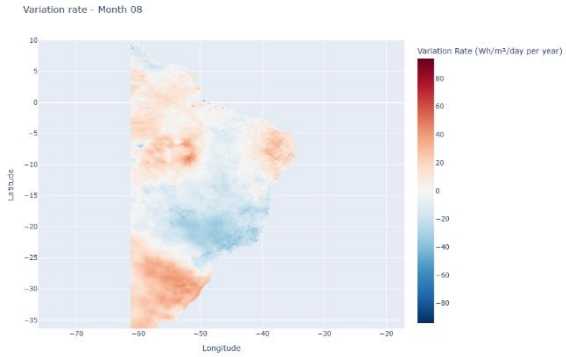

i) September

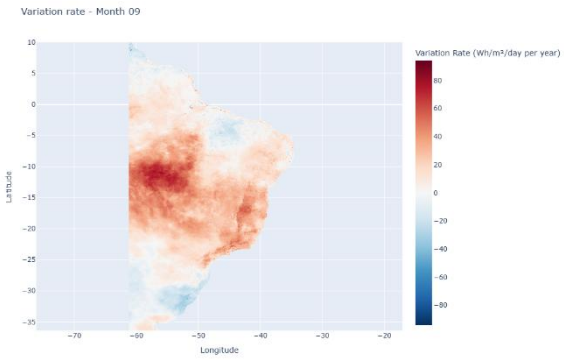

j) October

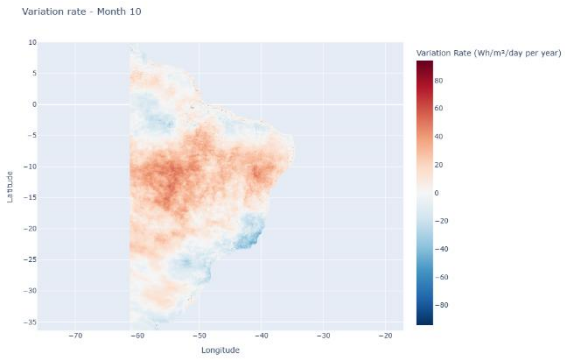

k) November

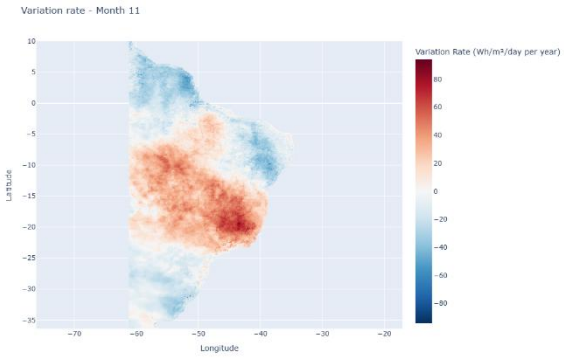

l) December

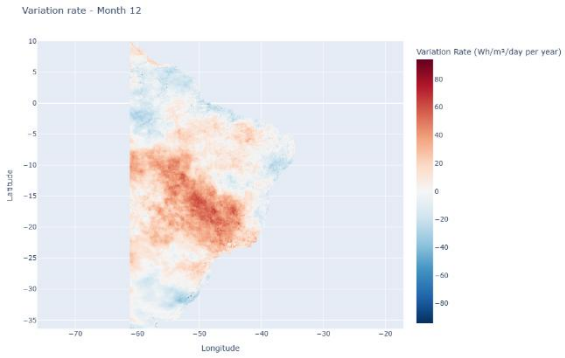

Source: Own Authorship, 2025

5 CONCLUSION

A thorough evaluation of the CAMS gridded solar radiation database in Brazil with a bilinear interpolation method has yielded some valuable insights into its performance and applicability for solar energy resource assessment. A comprehensive comparison with ground-based measurements at 11 stations revealed that the CAMS database generally tends to overestimate solar radiation, with some regional and seasonal variations, with an average nRMSE of 26.87%.

The analysis of seasonal patterns further revealed that the accuracy of CAMS data varies throughout the year, with higher discrepancies observed in the summer and the beginning of the autumn, a period characterised by increased cloud cover and rainfall in many parts of Brazil. Conversely, the database demonstrated stronger correlation with ground measurements during drier seasons, such as late winter and early spring. This seasonal variability underscores the necessity of incorporating local meteorological conditions into solar energy planning using the CAMS database.

A comparison of the CAMS Gridded and CAMS Time Series products was undertaken to determine the relative merits of each dataset in relation to location and specific application. In certain instances, the gridded data exhibited a closer approximation to ground measurements, even when employing a rudimentary interpolation method such as bilinear interpolation. Conversely, in other instances, the time series data demonstrated superior performance. This underscores the necessity for judicious selection of data sources and interpolation methods, particularly in regions characterised by complex terrain or highly variable weather patterns.

In order to enhance the accuracy and reliability of the CAMS Radiation Service, future research could involve the integration of hybrid models that combine satellite data with real-time ground measurements. Additionally, the incorporation of dynamic correction factors for cloud cover and atmospheric scattering could enhance the database's capacity to account for local variations. The implementation of these enhancements is expected to further enhance the utility of the CAMS Radiation Service as a valuable tool for the assessment of solar energy resources, particularly in regions characterised by significant weather variability.

The anomaly maps generated from the CAMS data provided a visual representation of the spatial and temporal variations in solar radiation across Brazil. These maps demonstrated a slight overall increase in mean solar radiation over the

years, with more pronounced changes observed in certain regions, such as the southeastern part of the country during the summer months. These findings suggest that climatological factors, such as the El Niño-Southern Oscillation, may be influencing solar radiation levels in certain areas. Beyond that, the trend maps illustrate the historical changes in solar radiation, with maximum values of 80 Wh/m^2/year recorded in specific regions.

In conclusion, it is evident that the CAMS gridded solar radiation database represents a substantial resource for large-scale solar energy assessments. The database's provision of data in a spatial distribution enables the utilisation of various interpolation methods as required. The incorporation of additional data sources or correction methods will ensure the database's continued effectiveness in supporting the planning and development of solar energy projects in Brazil and beyond.

REFERENCES

BSRN. BSRN Global Network Recommended QC Tests, V2.0. Available at: https://bsrn.awi.de/fileadmin/user_upload/bsrn.awi.de/Publications/BSRN_recommended_QC_tests_V2.pdf. Accessed on: 28 Mar 2025.

CAVALCANTI, Matheus Barbosa. Comparação de dados de GHI entre bases de dados de satélite, reanálise e estações solarimétricas da Rede SONDA. 2022.

COPERNICUS ATMOSPHERE MONITORING SERVICE. Available at: https://atmosphere.copernicus.eu. Accessed on: 15 Jan. 2025.

COPERNICUS ATMOSPHERE MONITORING SERVICE (CAMS). CAMS gridded solar radiation. Atmosphere Data Store (ADS). Available at: https://ads.atmosphere.copernicus.eu/datasets/cams-gridded-solar-radiation?tab=overview. Accessed on: 15 Jan. 2025.

COPERNICUS ATMOSPHERE MONITORING SERVICE (CAMS). CAMS solar radiation time-series. Atmosphere Data Store (ADS). Available at: https://ads.atmosphere.copernicus.eu/datasets/cams-solar-radiation-timeseries?tab=overview. Accessed on: 15 Jan. 2025.

EMPRESA DE PESQUISA ENERGÉTICA (EPE). Balanço Energético Nacional 2024. Available at: https://www.epe.gov.br/pt/publicacoes-dados-abertos/publicacoes/balanco-energetico-nacional-2024. Accessed on: 18 Fev. 2025.

ESPOSITO, Elena; LEANZA, Gianni; DI FRANCIA, Girolamo. Comparative analysis of ground-based solar irradiance measurements and Copernicus satellite observations. *Energies*, v. 17, n. 7, 2024. Article 1579. ISSN 1996-1073. DOI: https://doi.org/10.3390/en17071579. Accessed on: 03 Feb. 2025.

FERREIRA CORREA, L.; FOLINI, D.; CHTIRKOVA, B.; WILD, M. Trends in observed surface solar radiation and their causes in Brazil in the first two decades of the 21st

century. *Atmospheric Chemistry and Physics*, v. 24, p. 8797–8819, 2024. DOI: https://doi.org/10.5194/acp-24-8797-2024. Accessed on: 18 Mar. 2025.

FREIRE, Julliana Larise Mendonça; LIMA, Jeane Rafaele Araújo; CAVALCANTI, Enilson Palmeira. Análise de aspectos meteorológicos sobre o Nordeste do Brasil em anos de El Niño e La Niña. *Revista Brasileira de Geografia Física*, v. 3, n. 1, p. 429-444, 2011. Available at: https://www.researchgate.net/publication/322349719_Analise_de_Aspectos_Meteorologicos_Sobre_o_Nordeste_do_Brasil_em_Anos_de_El_Nino_e_La_Nina. Accessed on: 28 Mar 2025.

GG WEATHER. Oceanic Niño Index (ONI) - ENSO. Available at: https://ggweather.com/enso/oni.htm. Accessed on: 28 Mar 2025.

GOOGLE MAPS. Custom Map Viewer. Available at: https://www.google.com/maps/d. Accessed on: 14 Feb 2025.

GSCHWIND, B. et al. Improving the McClear model estimating the downwelling solar radiation at ground level in cloud-free conditions – McClear-V3. *Meteorologische Zeitschrift*, 2019. DOI: https://doi.org/10.1127/metz/2019/0946. Accessed on: 31 Mar 2025.

IQBAL, M. *An Introduction to Solar Radiation*. [s.l.]: Academic Press, 2012.

KOBLER, A.; ZUPAN, S.; KOCJAN, A. Comparison of spatial interpolation methods and multi-layer neural networks for different point distributions on a digital elevation model. *Geodetski Vestnik*, v. 57, n. 3, p. 523-543, 2013. Available at: http://doi.org/10.15292/geodetski-vestnik.2013.03.523-543. Accessed on: 10 Mar. 2025.

LEFÈVRE, M. et al. McClear: A New Model Estimating Downwelling Solar Radiation at Ground Level in Clear-Sky Conditions. *Atmospheric Measurement Techniques*, v. 6, n. 9, p. 2403–2418, 2013. DOI: https://doi.org/10.5194/amt-6-2403-2013. Accessed on: 31 Mar 2025.

LIEBMANN, Brant et al. Submonthly convective variability over South America and the South Atlantic convergence zone. *Journal of Climate*, v. 12, n. 7, p. 1877-1891, 1999. DOI: https://doi.org/10.1175/1520-0442(1999)012<1877:SCVOSA>2.0.CO;2. Accessed on: 28 Mar 2025.

LUND, Henrik; MATHIESEN, Brian; CONNOLLY, D.; ØSTERGAARD, Poul. Renewable energy systems – A smart energy systems approach to the choice and modelling of 100% renewable solutions. *Chemical Engineering Transactions*, v. 39, p. 1-6, 2014. DOI: https://doi.org/10.3303/CET1439001. Accessed on: 08 Mar 2025.

MIRANDA, D. R. et al. Quality Assurance Procedure for Solar Radiation at Minute Resolution. *EuroSun 2022: 14th International Conference on Solar Energy for Buildings and Industry*, 25-29 Sep. 2022, Kassel, Germany. DOI: https://doi.org/10.18086/eurosun.2022.15.04. Accessed on: 31 Mar 2025.

NOTTON, Gilles; VOYANT, Cyril. Forecasting of intermittent solar energy resource. In: YAHYAOUI, Imene (Ed.). *Advances in Renewable Energies and Power Technologies*. Elsevier, 2018. p. 77-114. ISBN 9780128129593. DOI: https://doi.org/10.1016/B978-0-12-812959-3.00003-4. Accessed on: 03 Feb. 2025.

OLIVEIRA, Gilvan Sampaio de. *O El Niño e Você – O Fenômeno Climático*. São José dos Campos: Editora Transtec, 2001.

Our World In Data. Solar photovoltaic module price. 2024. Available at: https://ourworldindata.org/grapher/solar-pv-prices-vs-cumulative-capacity. Accessed on: 18 Jan. 2025.

PEREIRA, E. B. et al. *Atlas Brasileiro de Energia Solar*. 2nd ed. São José dos Campos: INPE, 2017. 80 p. Available at: http://doi.org/10.34024/978851700089. Accessed on: 03 Feb. 2025.

PONS, Xavier; NINYEROLA, Miquel. Mapping a topographic global solar radiation model implemented in a GIS and refined with ground data. *International Journal of*

Climatology, v. 28, p. 1821-1834, 2008. DOI: https://doi.org/10.1002/joc.1676. Accessed on: 13 Mar. 2025.

QI, Qinghai et al. Mapping of 10-km daily diffuse solar radiation across China from reanalysis data and a Machine-Learning method. *Scientific Data*, v. 11, 756, 2024. DOI: https://doi.org/10.1038/s41597-024-03609-1. Accessed on: 31 Mar 2025.

QU, Z. et al. Fast Radiative Transfer Parameterisation for Assessing the Surface Solar Irradiance: The Heliosat-4 Method. *Meteorologische Zeitschrift*, v. 26, p. 33-57, 2017. DOI: https://doi.org/10.1127/metz/2016/0781. Accessed on: 31 Mar 2025.

SALES, Vilane G.; STROBL, Eric; ELLIOTT, Robert J. R. Cloud cover and its impact on Brazil's deforestation satellite monitoring program: Evidence from the cerrado biome of the Brazilian Legal Amazon. *Applied Geography*, v. 140, 2022, p. 102651. ISSN 0143-6228. DOI: https://doi.org/10.1016/j.apgeog.2022.102651. Accessed on: 31 Mar 2025.

SANTOS, Reinan Viana de Almeida; RIFFEL, Douglas Bressan. Estimativa da irradiância direta, difusa e global utilizando células fotovoltaicas de referência em diferentes ângulos de inclinação. *Revista FT*, v. 27, n. 118, jan. 2023. DOI: https://doi.org/10.5281/zenodo.7570344. Accessed on: 14 Abr 2025.

SCHROEDTER-HOMSCHEIDT, M. et al. User's Guide to the CAMS Radiation Service (CRS) Status December 2021. Dec. 2021. p. 1–76. Available at: https://atmosphere.copernicus.eu/sites/default/files/2022-01/CAMS2_73_2021SC1_D3.2.1_2021_UserGuide_v1.pdf. Accessed on: 31 Mar 2025.

ŞEN, Zekâi; ŞAHİN, Ahmet D. Spatial interpolation and estimation of solar irradiation by cumulative semivariograms. *Solar Energy*, v. 70, n. 1, p. 57-64, 2001. DOI: https://doi.org/10.1016/S0038-092X(01)00009-3. Accessed on: 10 Mar. 2025.

SOUZA, E. B. de; AMBRIZZI, T. ENSO impacts on the South American rainfall during 1980s: Hadley and Walker circulation. *Atmósfera*, Ciudad de México, v. 15, n. 2, p. 105–120, 2002. Accessed on: 16 abr. 2025.

WANG, C. Atmospheric circulation cells associated with the El Niño–Southern Oscillation. *Journal of Climate*, v. 15, n. 4, p. 399–419, 2002. Accessed on: 16 Apr. 2025.

WEATHERSPARK. Climate and Weather Data for Brazil. Available at: https://pt.weatherspark.com/countries/BR. Accessed on: 28 Mar 2025.

WILCOX, S.; GUEYMARD, Chris. Spatial and temporal variability of the solar resource in the United States. *39th ASES National Solar Conference 2010 – SOLAR 2010*, v. 2, 2010. Available at: https://www.researchgate.net/publication/236314614_Spatial_and_temporal_variability_of_the_solar_resource_in_the_United_States. Accessed on: 31 Mar 2025.

YOSHIKANE, T.; YOSHIMURA, K. A downscaling and bias correction method for climate model ensemble simulations of local-scale hourly precipitation. *Scientific Reports*, v. 13, p. 9412, 2023. DOI: https://doi.org/10.1038/s41598-023-36489-3. Accessed on: 13 Mar. 2025.

APPENDIX A – GENERATED STATISTICS TABLES

Table 2 – DHI 15 min statistics

Stations	Bias (W/m²)	bias_perc (%)	RMSE (W/m²)	RMSE_perc (%)	coef_p
Petrolina gridded	9.34	5.16%	73.63	40.64%	0.85
Petrolina time-series	7.61	4.20%	82.42	45.49%	0.81
Sao Luiz gridded	51.34	20.78%	166.75	67.50%	0.62
Sao Luiz time-series	49.02	19.84%	172.65	69.88%	0.59
Sao Martinho da Serra gridded	-0.54	-0.39%	74.03	53.98%	0.80
Sao Martinho da Serra time-series	-0.09	-0.07%	72.04	52.54%	0.82
Ourinhos gridded	-16.90	-11.74%	77.44	53.79%	0.81
Ourinhos time-series	-16.64	-11.56%	75.16	52.21%	0.83
Brasilia gridded	5.35	3.29%	70.40	43.29%	0.86
Brasilia time-series	2.54	1.56%	83.83	51.54%	0.81
Natal gridded	28.65	15.45%	113.58	61.25%	0.65
Natal time-series	13.34	7.19%	116.24	62.68%	0.63
Cachoeira Paulista gridded	2.19	1.38%	65.17	41.14%	0.87
Cachoeira Paulista time-series	2.01	1.27%	71.05	44.85%	0.85
Florianopolis gridded	17.95	11.28%	72.60	45.65%	0.85
Florianopolis time-series	13.30	8.36%	75.09	47.22%	0.83
Patos gridded	16.60	9.47%	96.84	55.24%	0.76
Patos time-series	13.47	7.68%	100.40	57.27%	0.74
Coremas gridded	2.36	1.49%	65.58	41.32%	0.85
Coremas time-series	2.27	1.43%	67.92	42.79%	0.85
Sao Joao do Rio do Peixe gridded	4.04	2.44%	66.33	40.01%	0.86
Sao Joao do Rio do Peixe time-series	6.01	3.63%	65.55	39.54%	0.87

Table 3 – DNI 15 min statistics

Stations	Bias (W/m²)	bias_perc (%)	RMSE (W/m²)	RMSE_perc (%)	coef_p
Petrolina gridded	-57.06	-14.44%	213.36	54.00%	0.81
Petrolina time-series	-50.91	-12.89%	231.80	58.67%	0.78
Sao Luiz gridded					
Sao Luiz time-series					
Sao Martinho da Serra gridded	-19.62	-4.33%	187.14	41.30%	0.88
Sao Martinho da Serra time-series	-23.39	-5.16%	180.35	39.80%	0.89
Ourinhos gridded	-11.20	-5.38%	167.24	80.33%	0.85
Ourinhos time-series	-13.89	-6.67%	161.27	77.46%	0.87
Brasilia gridded	-69.33	-15.62%	205.42	46.29%	0.85
Brasilia time-series	-58.23	-13.12%	226.80	51.11%	0.81
Natal gridded	-88.58	-21.76%	229.85	56.47%	0.76
Natal time-series	-72.40	-17.78%	230.70	56.67%	0.75
Cachoeira Paulista gridded	-52.95	-13.45%	176.21	44.75%	0.89

Cachoeira Paulista time-series	-56.08	-14.24%	188.47	47.86%	0.88
Florianopolis gridded	-37.88	-12.47%	172.03	56.64%	0.89
Florianopolis time-series	-33.79	-11.12%	181.27	59.68%	0.88
Patos gridded	-63.56	-14.96%	192.27	45.25%	0.85
Patos time-series	-59.85	-14.08%	200.40	47.16%	0.84
Coremas gridded	-43.37	-9.57%	198.67	43.83%	0.83
Coremas time-series	-37.30	-8.23%	199.41	43.99%	0.83
Sao Joao do Rio do Peixe gridded	-32.65	-6.76%	182.07	37.68%	0.85
Sao Joao do Rio do Peixe time-series	-40.02	-8.28%	176.26	36.48%	0.87

Table 4 – GHI 15 min statistics

Stations	**Bias (W/m²)**	**bias_perc (%)**	**RMSE (W/m²)**	**RMSE_perc (%)**	**coef_p**
Petrolina gridded	-30.91	-6.72%	126.50	27.51%	0.92
Petrolina time-series	-28.68	-6.24%	134.64	29.28%	0.91
Sao Luiz gridded	-41.62	-10.31%	140.00	34.69%	0.90
Sao Luiz time-series	-42.17	-10.45%	147.21	36.48%	0.89
Sao Martinho da Serra gridded	3.69	0.92%	106.70	26.59%	0.94
Sao Martinho da Serra time-series	2.72	0.68%	101.00	25.17%	0.95
Ourinhos gridded	-26.33	-6.54%	127.51	31.65%	0.91
Ourinhos time-series	-26.96	-6.69%	118.38	29.38%	0.93
Brasilia gridded	-25.79	-5.70%	140.55	31.04%	0.90
Brasilia time-series	-20.56	-4.54%	153.25	33.84%	0.88
Natal gridded	-20.92	-4.36%	104.70	21.82%	0.95
Natal time-series	-23.26	-4.85%	99.47	20.73%	0.95
Cachoeira Paulista gridded	-15.46	-3.76%	108.65	26.39%	0.94
Cachoeira Paulista time-series	-17.59	-4.27%	112.01	27.21%	0.94
Florianopolis gridded	-4.98	-1.39%	105.95	29.55%	0.94
Florianopolis time-series	-5.94	-1.66%	109.58	30.56%	0.93
Patos gridded	-12.19	-2.35%	106.54	20.53%	0.95
Patos time-series	-13.29	-2.56%	108.27	20.86%	0.95
Coremas gridded	-18.59	-3.69%	113.07	22.44%	0.94
Coremas time-series	-13.64	-2.71%	111.54	22.13%	0.94
Sao Joao do Rio do Peixe gridded	-8.39	-1.61%	106.71	20.45%	0.95
Sao Joao do Rio do Peixe time-series	-12.14	-2.33%	102.01	19.55%	0.95

APPENDIX B – GENERATED RADIATION MAPS

In this appendix, all the monthly anomaly maps can be consulted. They are stored in the file ‘Anomaly_Maps.html ' which was attached together with the text document.